

Eberhard Karls University of Tübingen
Faculty of Information and Cognitive Science
Wilhelm-Schickard-Institute for Computer Science

Diploma Thesis Bioinformatics

Place Cells in the Rat Hippocampus in Virtual Environments

Anna Jasper

01.03.2010

Referees

Prof. Rosenstiel
Department for Computer Engineering
University of Tübingen

Prof. Mallot
Department of Cognitive Neuroscience
University of Tübingen

Mentor

Dr. Thiele
Department of Cognitive Neuroscience
University of Tübingen

Jasper, Anna:

Place Cells in the Rat Hippocampus in Virtual Environments

Diploma Thesis Bioinformatics

Eberhard Karls University of Tübingen

Declaration for the Diploma Thesis

I warrant, that the thesis is my original work and that I have not received outside assistance. Only the sources cited have been used in this draft. Parts that are direct quotes or paraphrases are identified as such.

Place, Date

Signature

Abstract

The phenomenon that place cells in the CA1 and CA3 region of the rat hippocampus increase their firing rate when the rat is in a certain location (the ‘place field’), is well known. When place cells were first discovered, they were interpreted as the neural correlates of spatial orientation, the cognitive map. Since that time many studies have tried to determine the factors influencing a place field and how rats use this system for navigation. Whilst these studies have revealed numerous findings, they were all done under laboratory conditions in small areas of about a few m². The question of how these cells behave in large areas comparable to the normal home range of a rat remains unanswered.

In 2005, the Department of Cognitive Neuroscience of the University of Tübingen developed a virtual reality setup for rodents. It consists of an air-cushioned Styrofoam ball serving as a 2D-treadmill and a virtual environment that is projected on a 360° toroidal screen. This setup provides the opportunity to record place cells in virtually unlimited areas and to investigate the behavior of place cells under these conditions. Previous studies have shown that the recording of place cells in this virtual reality setup is possible. For the present study it has been extended with an amplifier for acoustic signals to provide additional cues to the animal. It shows that the use of sound cues can increase the performance of the rats in the virtual reality setup but also that the complexity of learning a task is higher than in a real area. Additionally the recording of the same cell in a virtual and a real environment is possible. These results encourage further investigations on the firing activity of place cells in virtual environments under differing conditions, like changing the geometry, rotating landmarks or even within a constantly changing environment.

Acknowledgements

First I would like to thank Prof. Mallot of the Department of Cognitive Neuroscience and Prof. Rosenstiel of the Department of Computer Engineering for giving me the opportunity to do this diploma-thesis.

My special thank goes to my mentor Dr. Johannes Thiele for his encouragement, guidance and strong support and for the many things he taught me. I thoroughly enjoyed working with him.

Next I would like to thank Martina Schmoee-Seelich, especially for her help with the rats and the brain sections. I am very grateful to Rüdiger Sadler and Sonja Seeger-Armbruster of the Department of Neuropharmacology for helping me with the brain lesions and perfusions. Here my thank also goes to Ursula Pascht of the Department of Cognitive Neurology, Hertie-Institute Tübingen for doing the brain-sections with me.

I am thankful to Aleksandar Jovalekic for his help with the analysis of place cells and the building of the microdrives.

Last but not least, I would like to express my gratitude to my mother for giving me the opportunity for this work and for her support. Thanks also goes to my brother Jurij for turning our house into an extremely 'noisy zone' while I was writing this thesis. This was valuable experience on obstacles to be encountered in academic work. Hope you enjoy your new billiard and bar room!

Contents

List of Figures	vii
List of Tables	x
1 Introduction	1
1.1 Motivation	1
1.2 The Cognitive Map	2
1.3 Place Cells	3
1.3.1 Remapping	3
1.3.2 The Role of Geometry	4
1.3.3 Other Studies on Place Cells	5
1.4 The Laboratory Rat	6
1.5 Virtual Realities	8
1.6 Previous Work	11
2 Material and Methods	15
2.1 Subjects	15
2.2 Axona Microdrive	15
2.3 Self-Developed Microdrive	19
2.4 The Headstage	20
2.5 Spike Recording	21
2.6 Data Analysis	22
2.6.1 The Cut Window	22

2.6.2	The Fields Window	23
2.6.3	The Time Window	23
2.7	The Virtual Reality Setup	24
2.7.1	The Treadmill	24
2.7.2	The Control-PC	25
2.7.3	The Projection-System	25
2.8	Surgery	26
2.9	Brain Lesions and Perfusion	27
2.10	Sectioning and Nissl staining	28
3	The Virtual Circular Road	30
3.1	Motivation	30
3.2	Materials and Methods	30
3.2.1	The Virtual Environment	30
3.2.2	The Tracking System	32
3.2.3	The Experimental Room	32
3.2.4	Procedure	33
3.3	Results	34
3.4	Discussion	35
4	The Real Circular Road	36
4.1	Motivation	36
4.2	Materials and Methods	36
4.2.1	The Arena	36
4.2.2	The Tracking System	37
4.2.3	The Experimental Room	38
4.2.4	Procedure	39
4.3	Noise as Additional Cue	39
4.3.1	Results	39
4.3.2	Discussion	44

4.4	Electrophysiology	45
4.4.1	Results	45
4.4.2	Discussion	51
5	The Virtual Circular Arena	54
5.1	Motivation	54
5.2	Materials and Methods	54
5.2.1	The Virtual Environment	54
5.2.2	The Tracking System	55
5.2.3	The Experimental Room	56
5.2.4	Procedure	57
5.3	Noise as Additional Cue	58
5.3.1	Results	58
5.3.2	Discussion	65
5.4	Electrophysiology	68
5.4.1	Results	68
5.4.2	Discussion	71
6	Discussion	72
6.1	Comparison of the Microdrive Architectures	72
6.2	Electrophysiology	73
6.3	Comparing the performance in the real and the virtual environment	74
7	Conclusion and Outlook	76
	Bibliography	78
A	Circuit Diagrams for the Headstage	82

List of Figures

1.1	Remapping experiment	4
1.2	Influence of room geometry on place fields	4
1.3	Spatial task	5
1.4	Mean occupancy in different zones	6
1.5	Body representation in the somatosensory cortex of a rat	7
1.6	Salla della Prospettiv	8
1.7	Hassenstein (1961) treadmill	10
1.8	Treadmill for insects as published by Dahmen (1980)	10
1.9	Sample trajectories and recordings	12
1.10	Trajectory of a rat running in a fixed direction	12
1.11	Self-made microdrive	13
1.12	Microdrive purchased from Axona Ltd	14
2.1	Schematic view of the Axona microdrive	16
2.2	Axona microdrive with guiding cannula	17
2.3	Axona microdrive from top view	17
2.4	Axona microdrive with nail varnish	18
2.5	Finished Axona microdrive	18
2.6	Schmeatic view of self-developed microdrive	19
2.7	Self-developed microdrive	20
2.8	TL074CD Pin connections	21
2.9	Headstages	21
2.10	Tint Example	23

2.11	The virtual reality setup	24
2.12	Schematic view of the virtual reality setup	25
2.13	Dorsal and lateral view of the rat skull	26
2.14	Results of brain section I	29
2.15	Results of brain section II	29
3.1	Virtual circular road, side view	31
3.2	Virtual circular road, top view	31
3.3	Layout of Experimental Room	32
3.4	Illustration of Procedure	33
3.5	Sample trajectories	34
4.1	Real circular road arena	37
4.2	Headstage with IR-LEDs	37
4.3	Experimental room	38
4.4	Sample trajectories	40
4.5	Normalized time within different zones	41
4.6	Normalized distance within different zones	42
4.7	Mean times	42
4.8	Mean distances	43
4.9	Mean velocities	43
4.10	Mean times within silent zone	44
4.11	Non-place-specific cell, rat 004, September 16 th , 2009	46
4.12	Non-place-specific cell, rat 004, September 18 th , 2009	47
4.13	Non-place-specific cell, rat 021, January 7 th , 2010	48
4.14	Place cell, rat 021, January 4 th , 2010	49
4.15	Place cell, rat 694, October 16 th , 2009	50
4.16	Place cell, rat 694, October 17 th , 2009	51
5.1	Virtual circular arena, side view	55
5.2	Virtual circular road, top view	55

5.3	Layout of Experimental Room	56
5.4	Inference caused by the white noise	57
5.5	Illustration of Procedure	58
5.6	Sample trajectories	59
5.7	Normalized time within different zones	60
5.8	Normalized distance within different zones	60
5.9	Reward-rate	61
5.10	Mean times	61
5.11	Mean distances	62
5.12	Mean velocities	62
5.13	Mean times within silent zone	63
5.14	Expected curves	64
5.15	Place cell, rat 021, January 4 th , 2010	69
5.16	Place cell, rat 021, January 7 th , 2010	70
A.1	Layout of circuit board I (top)	82
A.2	Layout of circuit board I (bottom)	83
A.3	Schematic view of circuit board I for the headstage	84
A.4	Layout of circuit board II (top)	85
A.5	Layout of circuit board II (bottom)	86
A.6	Schematic view of circuit board II for the headstage	87

List of Tables

4.1	T-test results	44
4.2	Recorded non-place-specific cells	49
4.3	Recorded place cells	50
5.1	Regression results reward rate	65
5.2	Regression results distance-ratio	65
5.3	Regression results time-ratio	65

Chapter 1

Introduction

1.1 Motivation

The home range of the wild rat varies between 0.33 m^2 and 1.83 m^2 with diameters between 86 m and 311m (Dowding and Murphy, 1994). These sizes differ significantly from the size of areas during place cells recordings. Therefore the question of how place cells behave within an area which has a comparable size to the home range of a freely moving rat arises. But due to technical limits, e.g. the recording cable, it seems impossible to run experiments within an arena having the size of the home range of a rat.

Another problem associated with the recording of place cells are the visual cues always given to the animal. Although it might be possible to reduce the number, there will always be some cues - maybe some not seen or smelled by the experimenter - helping the animal to determine its location.

The advantage of a virtual reality as opposed to the classical experiments performed in arenas of very limited size is that it is possible to do experiments in virtually unlimited environments under strongly controlled conditions. And – and this might be an advantage especially for cell recordings – the animal stays within the same place.

Putting this all together it is expected that recording place cells in virtual environments offers an opportunity to investigate how place cells behave within large areas, such as the home range of a wild rat.

1.2 The Cognitive Map

Today the word “*map*” is a commonly used term normally understood as some type of geographical abstraction.

*“Entry Word: **map***

Function: noun

Meaning: an illustration of certain features of a geographical area

(Merriam-Webster, 2007)

But the word “*map*” is not limited to a geographical context, like the map of the world. When asking different people what a map is and what kind of maps they know, the mathematician will tell you something about planar maps, the geologist something about contour maps, the computer scientist about bit-maps, the oceanographer about a gravity map and at the end you’ll meet a neuropsychologist and he tells you something about the cognitive map. As we focus here on neurophysiology, the next question would be “What is a cognitive map?”.

The origin of this term goes back to Edward Tolman (1886 – 1959), an American philologist. He described a cognitive map as

“...and it is this [the cognitive map] tentative map, indicating routes and paths and environmental relationships, which finally determines what responses, if any, the animal will finally release” (Tolman, 1948)

Therefore according to Tolman, a “cognitive map” is a geographical map in one’s mind. In 1948 he performed several experiments with rats in a maze. First he let the rats explore a maze where food was placed on specific places when they were not hungry. In the next session he put the rats into the maze when they had been food deprived. He showed that the rats were able to run directly towards the feeding places. Although one argumentation could be that the rats simply learned where the feeding places were. But according to Watson & Pavlov, learning is formed by reward and punishment. Hence in first session, the rat was neither rewarded (the rat was not hungry, it was not interested in the food) nor punished. So another explanation could be that the rats kind of “formed” a map in their mind and were therefore able

to remember were the food places were. Tolman called this form of learning ‘latent learning’ and proposed that the rat must have built up a representation of the spatial properties of its surroundings in its mind – the ‘cognitive map’.

Later on, in 1971, O’Keefe and Dostrovsky (1971) found cells in the CA1 and CA3 layer of the rat hippocampus which increased their firing rate dramatically as long as the rats stayed within a certain area. They thought that a system consisting of those cells could be the neural correlates of a cognitive map. They named these cells “place cells”. The location in which the cell increases its firing rate is called “place field”.

1.3 Place Cells

Today it is known that place cells are pyramidal complex-spike neurons found in the CA1 and CA3 regions of the hippocampus (Fox and Ranck, 1981). Assuming that a large number of place cells exist within the hippocampus, their fields might cover or map every given environment. This idea supports the hippocampus’ involvement in spatial mapping.

For the past 40 years several experiments have shown that place cells respond to changes in the environment. These can be changes in color Muller and Kubie (1987), odor (Anderson and Jeffery, 2003) and geometry O’Keefe and Burgess (1996) of the perceived environment (Lever et al., 2002) or a change of position in the experimental room (Hayman et al., 2003; Leutgeb et al., 2005), just to mention a few. These changes result in a place field on a different location (remapping), change in the maximum firing rate, change in the shape and size of the place field, development of a second or even a third place field or even disappearance of the place field.

In the following paragraph some basic experiments will be described.

1.3.1 Remapping

The basic set-up for a remapping experiment is an experimental area with a colored cue card. After a place field has been identified, the rat is removed and the position of the cue card is changed. When the rat is placed back into

the experimental area the place fields will rotate so as to maintain its position relative to the cue card (see figure 1.1). For details see Muller and Kubie (1987) or Bostock et al. (1991).

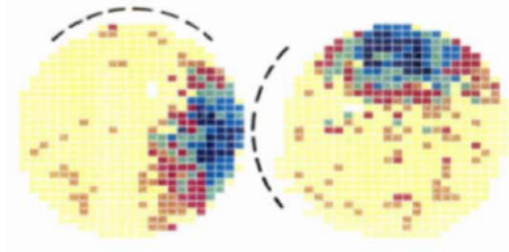


Figure 1.1: Remapping experiment: the dashed black line indicates the position of the white cue card (Bostock et al., 1991)

1.3.2 The Role of Geometry

O'Keefe and Burgess (1996) studied the influence of the geometry of the environment on the size and shape of a place field. They recorded place cells in four rectangular boxes that differed only in one of the sides (61 cm x 61 cm, 61 cm x 122 cm, 122 cm x 61cm and 122 cm x 122 cm). Their results showed that most of the place fields kept either a certain distance to a wall (see figure 1.2 a) or relative distance to two walls within the box (see figure 1.2 b)

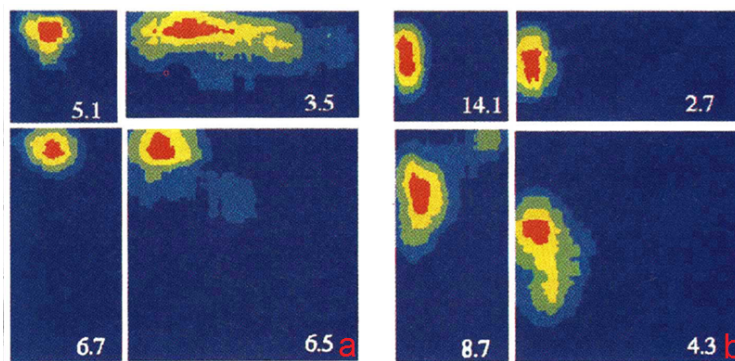


Figure 1.2: Two place cells recorded in different shaped environments. a) the place field has a fixed distance from the west and north wall b) the place field has a fixed distance from the west-wall and a fixed ratio of the distance between north and south (O'Keefe and Burgess, 1996, adapted)

1.3.3 Other Studies on Place Cells

In 2004 a study was published where Kentros et al. (2004) did place cell experiments with mice. In one experiment, the mice were suddenly exposed to loud noise and bright lights. In order to turn off the noise and the lights, the mice had to run to an unmarked goal region, which could be accurately located only by triangulating the arena cues. Figure 1.3 shows the experimental design.

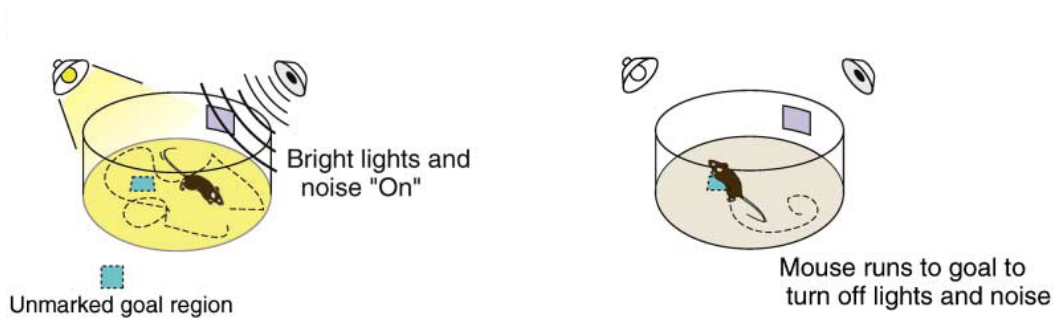


Figure 1.3: Experiment design of the spatial task (Kentros et al., 2004, adapted)

What they found was, that the mice did not only learn to turn off the noise and lights, also the place fields were significantly more stable when the mice performed a task compared to the stability of the place field when the mice performed no task.

Taking this as an onset Hayman et al. (2008) used white noise as a negative enforcer to keep rats out of a specific area. However Hayman et al. (2008) did not want the white noise to become a spatial cue. They achieved this by developing a fuzzy boundary, so the rats did not know when exactly the noise would sound. Therefore the arena was divided into three zones: a silent zone, a noisy zone and an adjustment zone between the silent and the noisy zone where the noise occurred based on the trajectory (inbound or outbound) of the rat. Figure 1.4 shows the mean occupancy in the three zones. The occupancy is defined as the time the rats spend in the zone divided by the size of the zone. It is quite obvious that the paradigm worked and the rats spent most of the time within the silent zone.

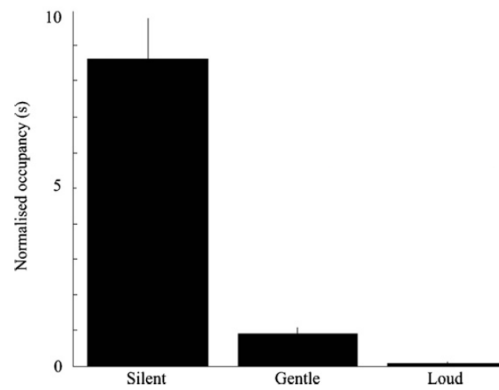


Figure 1.4: Results of Hayman et al. (2008), mean occupancy within the three different zones

1.4 The Laboratory Rat

For more than a century many experiments have been done using rats (*Rattus norvegicus*) as a model system. Although different strains are used for different purposes, they all go back to the wild brown rat. The most common used strains are Wistar, Sprague Dawley (both albino strains) and Long Evans (brown or black hooded). Animal experiments have to be designed according to the animals' behavior, physiology and anatomy. Therefore information relevant for this thesis about behavior and physiology of rats is given here.

Rats live in underground borrows and spend most of the time within a crowded underground environment that can be found in a forest underbrush, wetlands and grassy fields. In the city rats are most likely to be seen at underground train stations. Therefore it is not surprising that the rat's eye is good in gathering light but has bad optics. The retina consists of 1% cones and 99% rods (Vail, 1976) and does not possess a fovea. This is one of the reasons why rats are not fit as a model organism for behavioural tasks in experiments under normal laboratory light conditions. Regarding the rat's acuity it is with 1.0-1.1 c/d much lower than the acuity of humans, however similar to humans rats can detect single elements smaller than the acuity if the contrast is high enough. They can detect a 4% difference in a pattern of 0.1 to 0.2 c/d.

Rats hear within a frequency range of 0.25 kHz- 80 kHz (as comparison, young humans have a range of 0.02 kHz- 20 kHz). This shows that rats are able to detect ultrasound which lies within a frequency of 20 kHz- 1.6GHz. This needs to be considered when using computer monitors within the same room as the rat because they emit broadband ultrasonic sounds at a volume of 68- 84 dB which cannot be detected by humans (Sales et al., 1988).

The olfactory system of rats is well-developed. Their olfactory epithelium is complex and densely packed with olfactory neurons. Rats' communication is mediated through urine or other scent. Therefore it is obvious that the scent of other rats can influence the rat's behavior in an experiment.

The vibrissae system of a rat is highly developed and is a subject of high interest for many researchers throughout the world. This is not surprising when thinking of the poor performance of a rat's visual system. Besides the vibrissae system, nose and mouth, forepaws, and sinus hairs on the wrists are particularly well-represented in the somatosensory cortex. Figure 1.5 shows the importance of the systems. In fact rats can detect the position and distance of an object as well as the size and even the texture using their vibrissae.

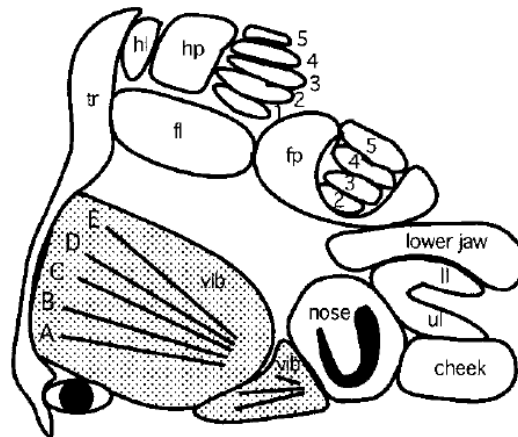


Figure 1.5: Body representation in the somatosensory cortex of a rat: f - foot; fl - flank; fp - forepaw; g - glabrous; hl - hind limb; hp - hind paw; ll - lower lip; ul - upper lip; t - tail; tr - trunk; vib - vibrissae (whiskers); A-E - individual vibrissae representations; 1-5 - paw digits (Geary and Huffman, 2002)

1.5 Virtual Realities

Albert Einstein (1879 – 1955) once stated “*Reality is merely an illusion, albeit a very persistent one*”.

An example of how true this statement is can be found in the “Villa Farnesia”.

In 1515 Baldassare Peruzzi, an Italian architect and painter, designed and built the Villa Farnesia for Agustino Chigi. The villa contains a room, the “Sala della Prospettiv” (engl. Hall of Prospective) in which the visitor gets the impression of being in hall surrounded by dark, veined marble piers and columns with gilded capitals that incorporates the actual veined marble door frames in the room. Through the columns the visitor can look out to a painted terrace and roofs of the City Rome. As can be seen in figure 1.6, it is almost impossible to perceive where the real marble ends and the illusion begins.



Figure 1.6: Sala della Prospettiv

This illusion can only be perceived when the visitor stands on a certain place revealing the right perspective. Intuitively you would think the intentions of

this room has something to do with perspective. Especially when considering that the mathematics behind perspective painting was first published around 1435 in Leon Battista Alberti's treatise "De pictura/Della Pittura" (Alberti, 1435) and perspective painting became an integral part of the quattrocento art period (fifteenth century) and still occupied the minds of many artists in the cinquecento period. But obviously Peruzzi chose the title of this room to indicate the futuristic quality.

The uniqueness of the room and the visual illusion it provides, suggests that the artist had in mind that in the future working with illusions would become very popular and indeed he was right. As the illusion arises only when the visitor stands in a well defined place of the room, one could say that this room was one of the first virtual realities.

Today, almost 500 years later, virtual realities (VRs) are not unique anymore. They are used in many fields like training pilots in flight simulators, automobile prototypes are ergonomically tested using VRs and even architecture-visualizations deploys VRs. Also in research VR is of growing importance and widely used. The advantage of using VRs lies in the extremely controlled conditions under which an experiment can be performed and the unlimited space available. Especially in neuroscience, VRs provide a good tool to investigate cognitive skills.

A wide range of VRs exists. In most experiments the testing person is in front of a large screen or wears a so called head-mounted-display (HMD). A HMD is a display device with an optic display in front of one or both eyes. Although these devices allow experiments to be executed under extremely controlled (visual) conditions, when the experiment involves action of the testing person like walking around, the area the person can walk in is limited by the size of the experimental room. Therefore it is not surprising that a HMD is often used together with an omnidirectional treadmill to provide unlimited sized areas.

When experimenting with animals using virtual reality, other approaches than with humans are required. Animals will not stay in front of a screen or wear a HMD while walking on an omnidirectional treadmill.

In 1961 Hassenstein developed a treadmill for insects to observe their locomotion behavior (Hassenstein, 1961). The treadmill consisted of six straws and three junctions. The straws were connected so that each three straws met in a junction. This is illustrated in figure 1.7.

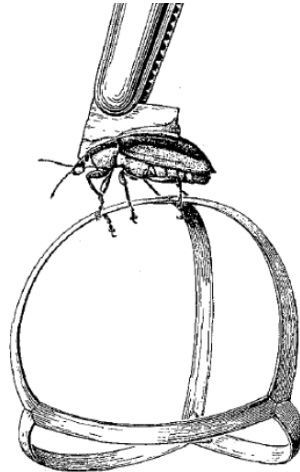


Figure 1.7: A fixated weevil walking on the treadmill (Hassenstein, 1961)

In 1980 Hansjürgen Dahmen presented a treadmill consisting of a small polystyrene sphere which was supported by an air cushion in a half spherical mould (Dahmen, 1980)(see figure 1.8).

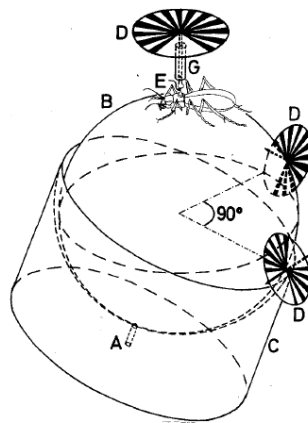


Figure 1.8: treadmill for insects as published by Dahmen in 1980. A=air supply, B= Styroporball, C= 'air cup', D= film disk with spoke pattern, E = elastic nylon thread, G = glass tube with needle (Dahmen, 1980)

Taking this as an onset, in 2005 Christian Hölscher published the design of a treadmill for rodents which also included a projection system for projecting a

virtual environment (Hölscher et al., 2005). Although it seems quite tempting to have a virtual reality setup for rodents or other animals, one has always to remember that animals might have a different vision system and might use other senses to be able to manage daily situations. Also, although the projection might be on a 360° toroidal screen, it remains 2-dimensional and therefore the stereo disparities are not correctly displayed. The recommendation here is to always run some basic navigation experiments to show whether and how the animals are able to navigate in this virtual reality.

1.6 Previous Work

In 2005 Hölscher et al. (2005) published a paper showing that rats are able to navigate within virtual environments. They designed a virtual environment where cylinders (50 cm diameter and 80cm in height) were placed in regular pattern in 20 cm above the ground with a distance of 2m. The rats were rewarded with sugar water every time they entered the area below a cylinder. For comparison a real arena was taken where three cylinders (20 cm diameter, 50 cm in height) were suspended from the ceiling about 40 cm above the ground. Reward was given only below one of these cylinders. Hölscher et al. (2005) showed that the rats were able to learn they will be rewarded under the cylinders.

Based on this publication Schnee (2008) designed several navigational tasks for rats based on this setup including one where he recorded cells from the CA1 region of the hippocampus while the rat was walking on a circular road. The results can be seen in figure 1.9.

As can be seen from figure 1.9, Schnee was able to record cells with a place-specific firing in the virtual environment.

During his diploma thesis in 2008, Aleksandar Jovalekic (2008) tried to reproduce the results from Aleksander Schnee (2008). Although he was able to record place cells in real arenas, recording in the virtual reality setup proved more difficult. His experimental design was comparable to Aleksander Schnee's. Jovalekic taught the rats to walk on a circular road. For every meter they walked on the road, a reward was given. As soon as they left the

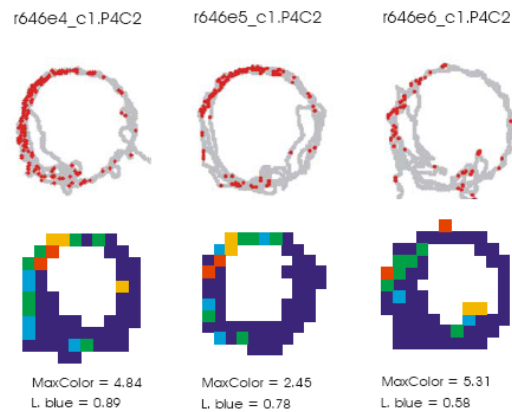


Figure 1.9: Sample trajectories and recordings from CA1 region. The grey cycles show the trajectories of the rats, red dots indicate the spikes. In the second line the density map displayed. (Schnee, 2008)

road they were punished with a short air puff. One of the main problems was that the rats sometimes started to run into fixed directions instead of following the circular road (see Figure 1.10). This problem has also been observed previously by Schnee (2008).

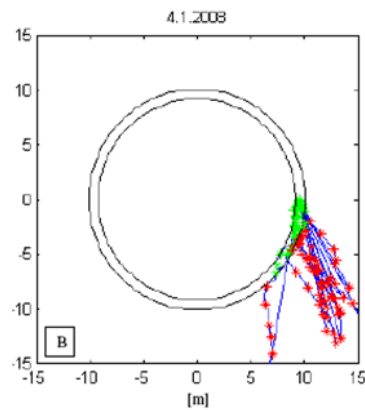


Figure 1.10: Trajectory of a rat running in a fixed direction (Jovalekic, 2008)

Another problem Jovalekic (2008) encountered was that the cells were not stable over multiple sessions. It is speculated that the reason lies in the architecture of the microdrive. The tetrodes are fixed to guiding cannulae which in turn are connected via a wire to a screw between the head and a nut. Although this architecture has the advantage that all four tetrodes can be adjusted individually, there might still be some tolerance between the screw head and the nut, allowing the tetrodes to change position without the screw being turned. For construction details see Chapter 2.

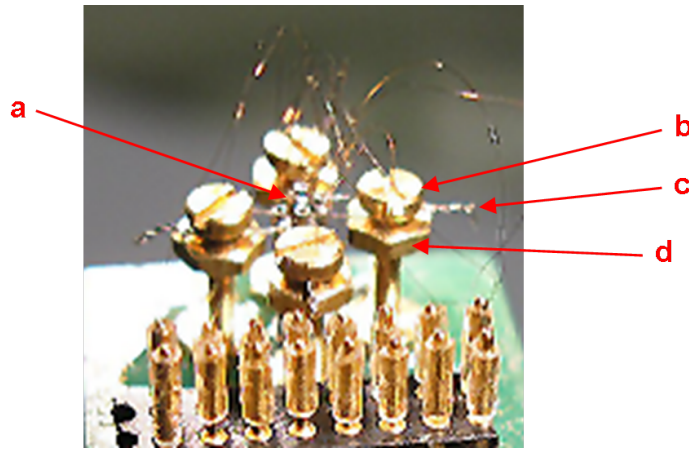


Figure 1.11: Picture of the microdrive showing the tolerance between the screw head and the nut a) guiding cannulae for tetrodes b) screw head c) wire connecting the cannulae with the screw d) nut

Considering these problems this thesis will test two new ideas.

First as mentioned in chapter 1.2. Kentros et al. (2004) not only showed that with the use of loud noise animals navigate to a certain area. The fact that the mice are performing a task (turning off the noise and lights) leads to more stable place fields. That rats can be kept out of a certain area using white noise has been shown by Hayman et al. (2008). Regarding the fixed-direction problem and the instability of the place cells, the use of white noise in combination with the virtual reality setup is obvious.

However if the instability of the place field is caused by the architecture of the microdrives it won't be resolved by letting the animals perform a task. So second different microdrives will be used. The new microdrives consist mainly of a precision screw and a frame holding the screw. The advantage of this technique is that the precision screw has a very fine pitch thread and the

guiding cannula and therefore the tetrodes are directly attached to the screw, disabling tolerance. The disadvantage of this architecture is that it does not allow moving tetrodes individually. A picture of this microdrive bought from Axona Ltd (St. Albans, UK) can be seen in figure 1.12.

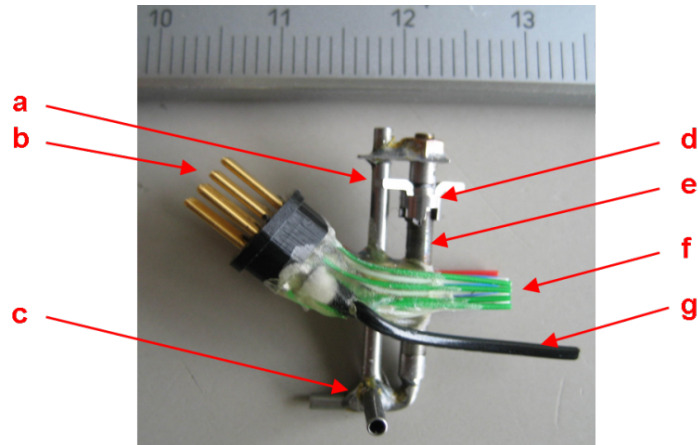


Figure 1.12: Microdrive purchased from Axona Ltd. a) frame holding the precision screw b) connector to the headstage c) base for embedding the microdrive into cement d) turner for precision screw e) precision screw f) microdrive wires g) ground

Chapter 2

Material and Methods

2.1 Subjects

Subjects were five male Long Evans rats purchased at the age of 10 weeks. Two rats (004, 694) were from the Charles Rives Laboratories and three (020, 021, 025) from the Janvier Laboratories. The rats were kept in groups of 2-4 rats in macrolon cages Type IV (Ehret Lab) until surgery. To prevent the animals from hurting each other, the rats were isolated after surgery. An additional wall was placed in the cages to ensure the animals would not get stuck in the bars with the microdrive. The rats received water ad lib and were fed daily with 20g of standard rodent food pellets.

2.2 Axona Microdrive

Two of the five microdrives used were purchased from Axona Ltd, St. Albans, UK. One was delivered with connector, the other without. The microdrive itself consists of a precision screw with a pitch of 200 μm and a frame holding the screw. The frame has a base to embed the microdrive in the cement. Figure 2.1 illustrates the assembly of the microdrive.

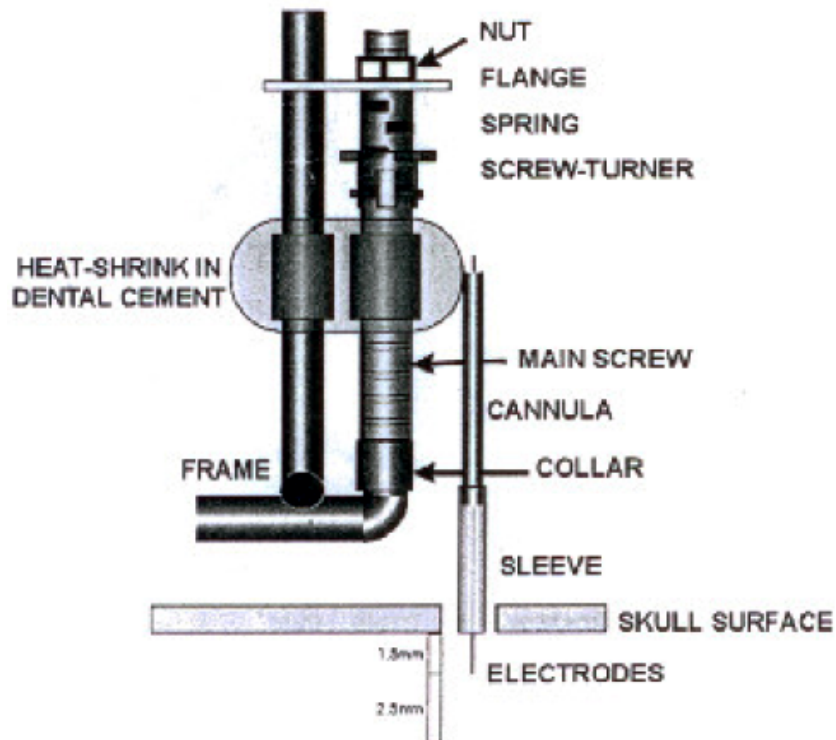


Figure 2.1: Schematic view of the Axona microdrive (Axona, 2009)

Before connecting the tetrodes to the microdrive, the guiding cannula has to be attached to the sleeve, see figure 2.2. After that the microdrive can be wired up by putting all four tetrodes into the cannula and fastening them there with a tip of superglue to the cannula. Then the wires of the tetrodes are wrapped around the loose ends of the microdrive's wires (see figure 2.3). Next, the wired connections of the tetrodes to Microdrives are coated with conductive silver paint. When the paint is dry, it is then coated with nail varnish for isolation (see figure 2.4). The wires are folded to the centerline and isolated with nail varnish again (see figure 2.5). For details on the assembly process see Axona (2009).

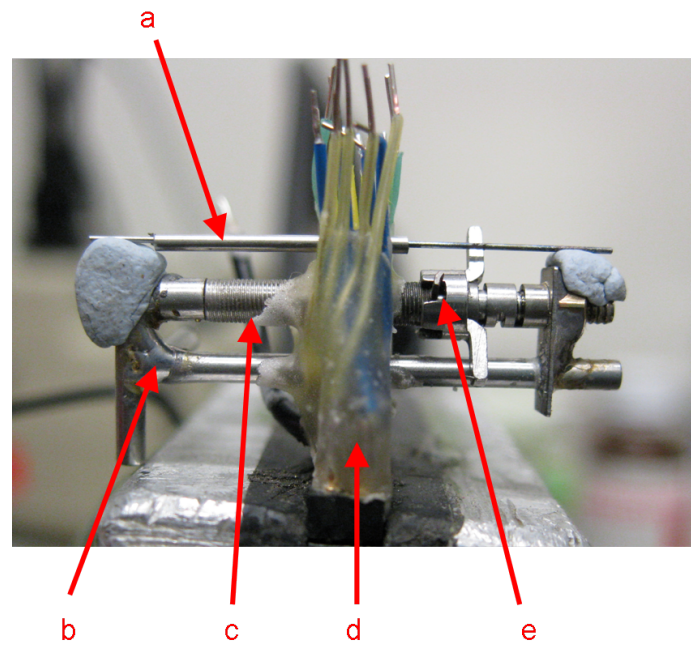


Figure 2.2: Axona microdrive with guiding cannula a) guiding cannula b) frame c) screw d) connector with microdrive wires e) screw-turner

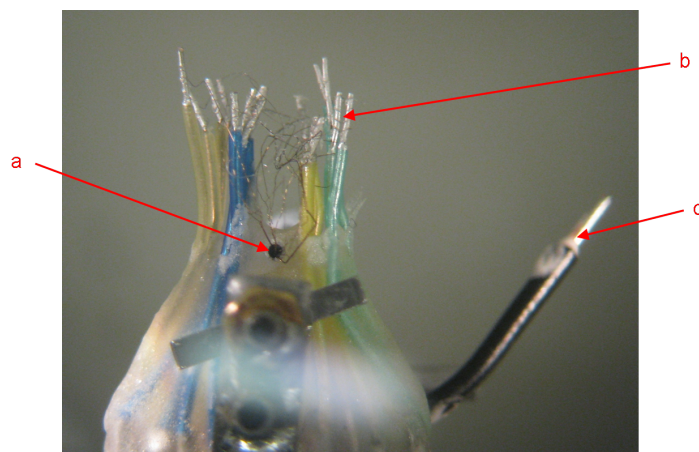


Figure 2.3: Axona microdrive from top view a) guiding cannula with tetrodes b) tetrode wires are warped around microdrive wires c) ground cable

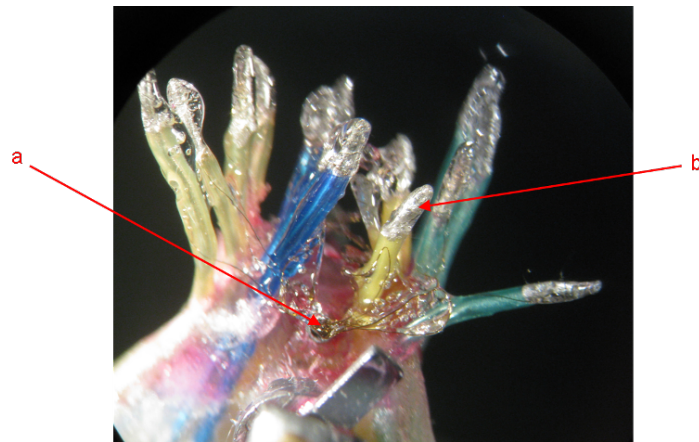


Figure 2.4: Axona microdrive with nail varnish around the wires a) guiding cannula with tetrodes b) nail varnish covered microdrive wire with wrapped tetrode wire

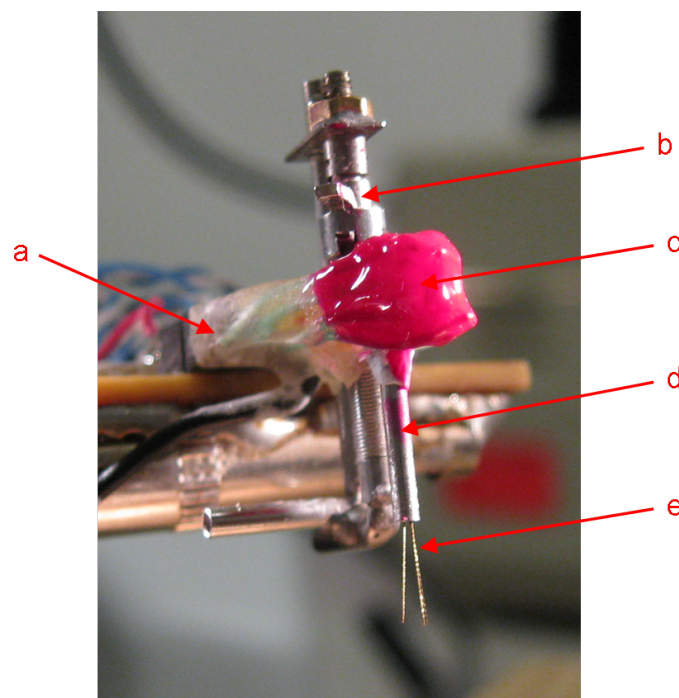


Figure 2.5: Finished Axona microdrive a) connector b) screw-turner c) microdrive wires covered with nail varnish d) sleeve e) tetrodes

2.3 Self-Developed Microdrive

Three of the five microdrives deployed were constructed in our laboratory. The basic construction was designed by Dr. Hansjürgen Dahmen. It was first modified by Omar Libchick during his lab-rotation job and then by Aleksandar Jovalekic for his diploma thesis. For construction details please see Libchik (2008) and Jovalekic (2008). The microdrive consists of four guiding cannulae, one for each tetrode. The tetrodes are fixed to the cannulae using superglue. A wire is soldered to each cannula and twisted around the corresponding screw between the screw head and the nut. This allows separate up and down adjustment of each tetrode by turning the screw. The pitch of the screws is $250\ \mu\text{m}$. See figure 2.6 for a schematic view.

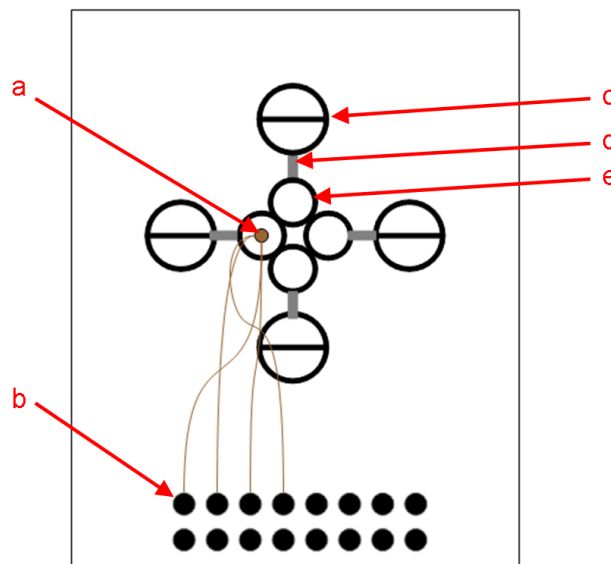


Figure 2.6: Schematic view of the microdrive a) example tetrode b) connector pins c) screw head d) connection wire e) guiding cannula for tetrodes

To be able to embed the microdrive in the cement, four wires (feet) are attached on the bottom side of the plate. To protect the tetrodes and screws a second plate is attached to the feet and the two plates are surrounded by a thin slice of plastic. See figure 2.7.

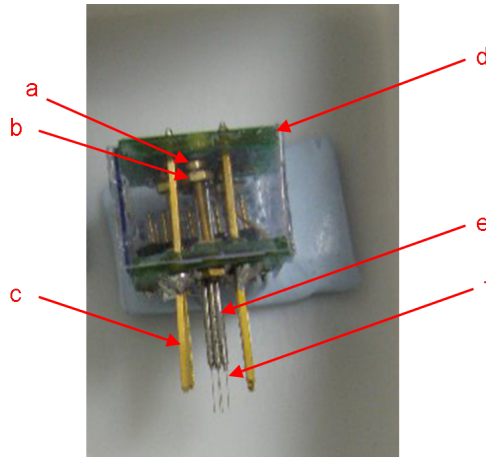


Figure 2.7: Self-developed microdrive a) screw head b) nut c) feet d) protection plate e) guiding cannulae f) tetrodes

2.4 The Headstage

Normally the Microdrive is connected to a preamplifier via a cable. To reduce the inference caused by cable flexion, a headstage is attached to the microdrive. This headstage amplifier interfaced the microdrive and the preamplifier. It is an impedance transformer based on an operational amplifier. Therefore it ensures that the high resistance from the electrode is converted into a low resistance and low impedance. Now that the microdrive has four tetrodes each equipped with four channels, 16 channels have to be processed. The headstage consists of two printed circuit boards. On each side of a board four of the 16 channels are processed with a TL074D low noise JFET-input operational amplifier. For pin connections, see figure 2.8

The V_{cc+} and V_{cc-} are set to $-12V$ and $+12V$ which is supplied by the recording computer. The resistors for the IR-LEDs are mounted on one board and the connector to attach the stick with the two IR-LEDs for the tracking is attached to the sides of both boards. For the corresponding circuit diagram see Appendix A.

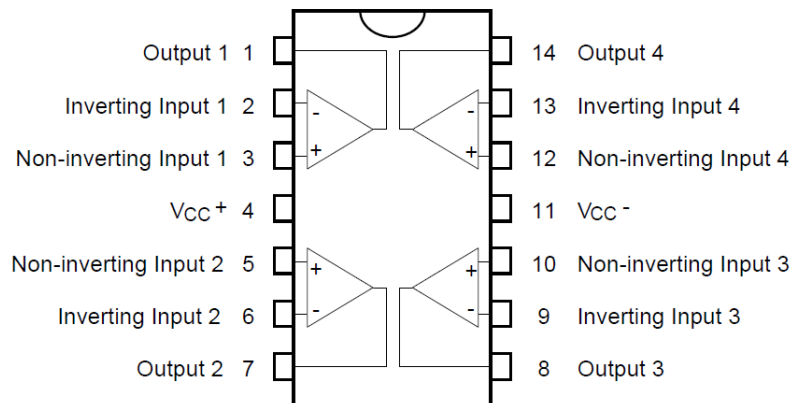


Figure 2.8: TL074CD Pin connections

Figure 2.9 shows the two used headstages.

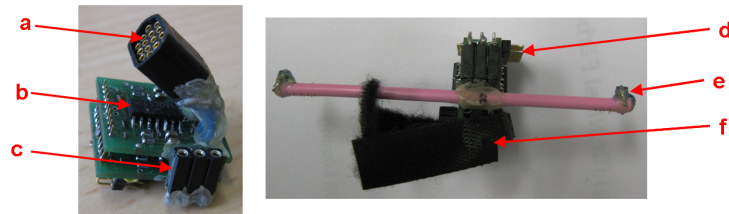


Figure 2.9: top: Headstage used for the Axona-Microdrive with Axona connector, bottom: headstage used for home made-microdrives as well as the Axona-Microdrive with precision multi-pin connector
 a) Axona female connector b) low noise JFET-input operational amplifier c) female connector for IR-LEDs d) male precision-multi-pin connector for cable e) IR-LEDs f) Velcro fastener for additional fixation of the microdrive

2.5 Spike Recording

As mentioned in the previous chapter, the signal is amplified prior to processing by the software. Here a preamplifier with a gain of 1000 was used. After being amplified the signal was split into a differential pair and was transferred to the recording computer. The advantage of splitting the signal is that the cable between the pre-amplifier and the recording computer can be up to 20 m in length while picking up marginal noise. The amplification of the recording software itself (Dacq2, Axona Ltd., St.Albans, UK) reaches from 0.25 to 64. Together with the pre-amplifier this resulted in amplifications from 250 to 64000. For the EEG recordings the lowpass filter (500 Hz cutoff) and the

50Hz notch filter was applied to the signal. For spike-recording a highpass filter (360Hz cutoff) was applied. The experimenter then chose a relative threshold for all channels. Next the gain for each channel was set manually. If one channel of a tetrode passed the threshold the signals of all four channels was stored within a time window of 200 μs pre- to 800 μs post threshold. The data was then stored into six files per session. The SET-file contained all settings, the POS-file the position tracking in pixel coordinates, and one file for each tetrode.

Additionally the software provides an interface to run scripts during the recordings phase. This was used to turn the noise on and off during experiment 2, and to synchronize the control computer for the virtual environment with the recording computer during experiment 3.

For more detailed information on the spike recording process and Dacq2 please see Axona (2004a).

2.6 Data Analysis

The clustering was performed with the Tint Cluster Cutting and Analysis Software (Axona Ltd, St.Albans, UK).The software provides three different analysis windows.

2.6.1 The Cut Window

The cut window is separated into two screens. On screen 1 multiple 2-dimensional feature plots are displayed. By default it displays the peak-through amplitude of the spikes on one channel against the ones of the other channel. This makes a total of six plots. For additional plotting parameters, the reader can refer to the manual (Axona, 2004b).

On screen 2 the summarized spikes as well as the average spike of one or more selected clusters can be seen. Spikes were clustered by visual inspection following the instructions in the manual (Axona, 2004b). Only if the summarized spikes within each channel had a similar shape and the average spikes showed a similar shape while having a different amplitude, the cluster was accepted. (see figure 2.10 a and b)

2.6.2 The Fields Window

In the fields window the density map for each cell could be seen. To identify a place-specific firing of a cell the averaged dwell time was chosen to be displayed in the density map. Also the interpolated smoothed path of the rat and the spikes of a selected cluster could be seen. This feature is important to see whether the cell fires only within a certain area or not (see figure 2.10 cand d)

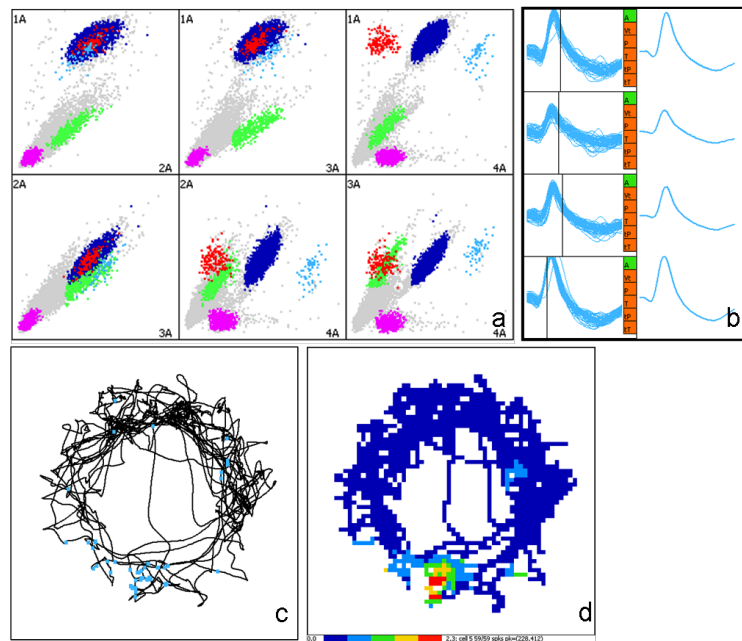


Figure 2.10: Tint Example: Recordings from rat 694 on September 19th, 2009 tetrode 2 a) shows the different clusters b) summarized spikes and average spike form of the light blue cluster. All spikes have the same form within the channel while across all channels the form is identical and the amplitude is different c) the interpolated path of the rat including all spikes (light-blue dots). As can be seen, the cluster includes very few spikes d) density map. The place field is in the lower middle of the area. The maximum firing rate is 2.3Hz (red).

2.6.3 The Time Window

Here autocorrelation was performed to ensure that the cell is not contaminated with other cells or noise. Also the autocorrelation was used to look for a periodic firing pattern. Here a time window of 1000 ms was chosen.

2.7 The Virtual Reality Setup

The virtual reality setup for rodents consists mainly of three parts, which will be briefly described in the following. For a detailed description see Hölischer et al. (2005) and Schnee (2008).

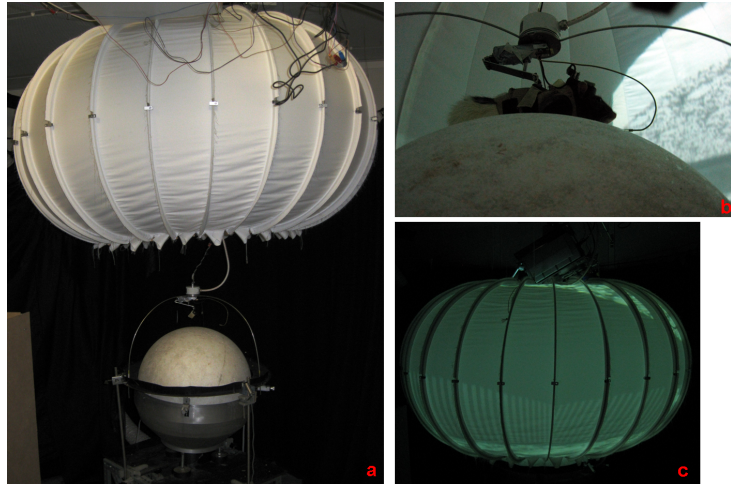


Figure 2.11: Virtual reality setup a) with lifted screen b) rat navigating in a virtual environment during experiment 3 c) running with lowered screen

2.7.1 The Treadmill

The animal runs on top of an air-supported spherical treadmill. The material is polystyrene, the weight 400g, and the diameter 50cm. The treadmill is located in a half-spherical mould with a diameter of 50.4 cm. The test rat wears a leather jacket which is attached to a small aluminum bracket using a Velcro fastener. This bracket allows the rat to lift and lower its body. The bracket is fastened to a magnet which is mounted to an angular increment encoder. Also a thin brass tube is affixed to the encoder for rewarding the animal with apple-juice. To track the animal's movement two x/y motion sensors (HDNS2000 Agilent, Palo Alto, CA, USA) are positioned in a 90° angle around the equator of the sphere. The used sensors are motion detectors found in common optical PC-mouse devices. The signals of the detectors are transferred to an incremental counter board (ACPI1719, ADDI-Data, Ottersweier, Germany) in the control-PC.

2.7.2 The Control-PC

The software controlling the virtual reality is written in C++. The projection and morphing of the virtual environment (VE) is done using Open Scene Graph, a 3D Graphics Toolkit. Besides the projection of the VE the control software controls of the rewarding system, turns the white noise on and off and initiates the recordings on the recording computer. For each session a log file documents the time, the local (within the projected environment) and global (overall) coordinates, the measurements of the angular increment encoder, a user defined bit and the smoothing direction.

2.7.3 The Projection-System

The rat is surrounded by a toroidal screen with a height of 80 cm and a diameter of 140cm. When the screen is lowered it visually covers a field of 360° of azimuth and -20° below to 60° above the horizon of the rat. The VE is projected with a common beamer (DDV 1800 Liesegang) via two planes and one angular amplification mirror on the toroidal screen.

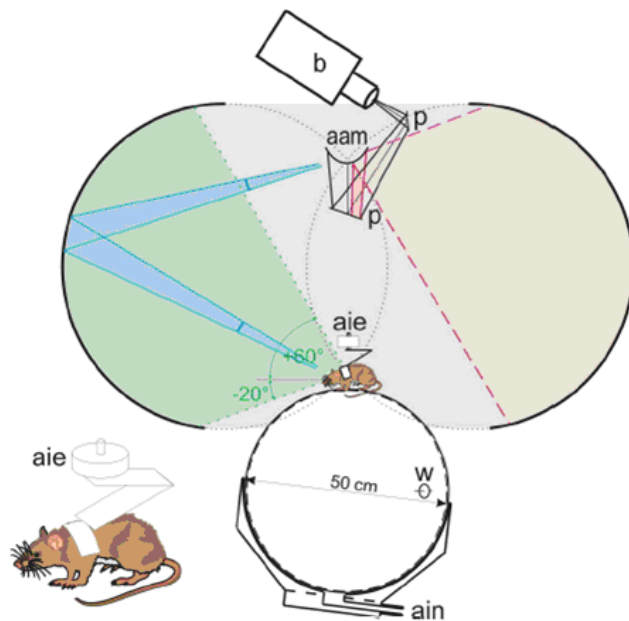


Figure 2.12: Schematic view of the virtual reality setup for rodents b) beamer p) plain mirror aam) angular amplification mirror aie) angular increment encode w) one of the two wheels preventing the sphere from rotating around the vertical axis ain) air inlet (Hölscher et al., 2005)

2.8 Surgery

The rats were anesthetized using 1 ml/kg Ketamine (Ketamin, Gräub Albrecht, Aulendorf, Germany) and 0.25 ml/kg Xylazine (Rompun, Bayer, Leverkusen, Germany). The injection was given intraperitoneally. When no toe-pinch-reflex could be observed the rat's head was shaved. The rat was then placed on a heating pad at 37°C and fixated in a stereotactic frame. To avoid dehydration and other damage to the eyes, they were covered with Bepathen (Bayer, Germany).

Then the scalp was cut open and the skull was washed with H₂O₂ until Lambda and Bregma could be identified (see Figure 2.13)

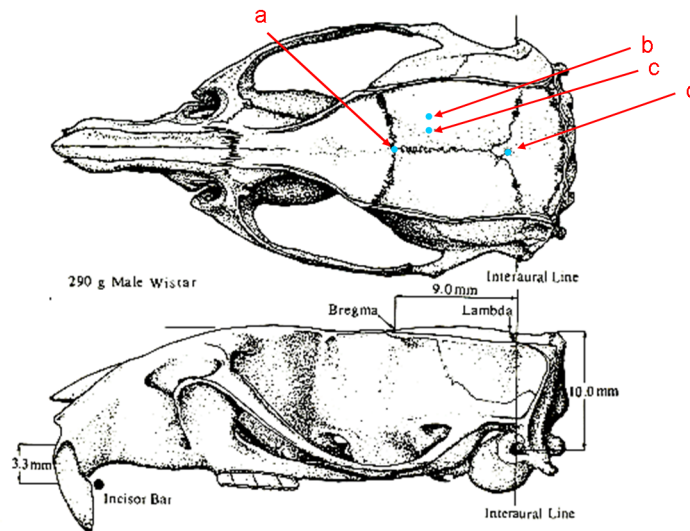


Figure 2.13: Dorsal and lateral view of the rat skull a) Bregma b) CA3 tetrode position c) CA1 tetrode position d) Lambda (Paxinos and Watson, 1998)

Taking Bregma as reference, a hole with a diameter of 2.3 mm was drilled into the skull at 3.4mm posterior and 1.6 mm lateral for the CA1 region (rats 004, 020, 021 and 025) or 3.4 mm posterior and 3mm lateral for the CA 3 region (rat 694) using a core drill. Before placing the microdrive 3-4 additional holes were drilled into the skull with a diameter of 1.2 mm serving as holes for the fixation screws. One of these screws provided a wire for grounding. Then the microdrive was positioned with a micro-manipulator above the hole and the brain surface was taken as reference to insert the tetrodes 1.6 mm into the tissue for the CA1 region, 2.2 mm for the CA3 region respectively. In order

to prevent the guiding cannulae and the tetrodes from getting stuck in the cement, they were covered with Vaseline (Vaseline, Caesar & Loretz, Hilden, Germany). This also kept the cement from entering the rat's brain. Then the exposed skull and the feet of the microdrive were covered with cement (Paladur, Heraeus Kulzer, Hanau, Germany). This fixated the microdrive to the screw which in turn served as a mechanical link between the cement and the skull.

After the surgery the rat was given 2 ml sodium-chloride solution subcutaneous and was put back into its home cage placed on the heating pad. The rat was provided with water but no food. After the rats started drinking, 20g rodent pellets were given. For the next two or three days (depending on the rat's behavior) the rat received 1 ml/kg Carprofen (Rimadyl, Pfizer GmbH, Germany) in a 1:10 dilution subcutaneous every 12 hours.

2.9 Brain Lesions and Perfusion

The brain lesions and the perfusions were done at the lab of Dr. Andreas von Ameln-Meyerhofer, Department of Neuropharmacology, University of Tübingen, Germany.

The rats were anesthetized with 10 ml/kg chloral hydrate intraperitoneally. After no toe-pinch-reflex was observed each tetrode was attached to a stimulus generator (STG 1001, Multichannel Systems, Germany). The stimulus used for the lesion was 1.5 periods (45s) of a square pulse lasting from -30 mV to 30 mV. Except for rat 021 all channels of a tetrode were used for lesion. For rat 021 only two channels per tetrode were used because the in this case deployed microdrive had a connector that was not compatible with the connector of the stimulus generator. Then phosphate-buffered paraformaldehyde (4g paraformaldehyde/100 ml 0.1M phosphate buffer) was perfused via heart injection to replace the blood and fixate the brain. After decapitation, the brain was removed and put into a 10% sucrose-fixation solution (10g sucrose / 100 ml phosphate-buffered paraformaldehyde) for two hours. After that the brain was cryoprotected with a 30% phosphate-buffered- sucrose solution (30g sucrose / 100ml 0.1M phosphate-buffered saline) and kept in the fridge at 4°C for five days.

2.10 Sectioning and Nissl staining

The brain sectioning for all four rats was done at the lab of Dr. Cornelius Schwarz, Department of Cognitive Neurology, Hertie-Institute, Tübingen, Germany.

On day six after the perfusion the brain was frozen in methybutan and fixated to the cryo-microtome using phosphate-buffered saline. Then it was cut into slices of 60 μm .

The slices were kept in well plates filled with 0.1M phosphate-buffered saline for the next two days. Then a Nissl staining was performed using the following protocol:

1. 10 min acetic acid (420 ml 99.9 % alcohol + 30 ml acetic acid)
2. 3 min distilled water
3. 6 min 0.1% Cresyl violet solution
4. 40 sec acetic acid (420 ml 99.9 % alcohol + 30 ml acetic acid)
5. 10 min 100% alcohol
6. 10 min Xylol

The slices were then covered with coverslips using DPX Mountant for Histology (Fluka, Sigma-Aldrich Chemie GmbH, Steinheim, Germany).

The results can be seen in figure 2.14 and figure 2.15

Figures 2.14 and 2.15 show the results from the brain section of rat 694. Here the microdrive was implanted to target the CA3 layer. As can be seen from figures 2.14 and 2.15 the entrance of the tetrodes is clearly visible. But it can also be seen that the end of the tetrodes are below the hippocampus and therefore in the thalamus. That the ends of the canals seen in figure 2.14 c and d and figure 2.15 c correspond to the end position of the end of the tetrode can't be assured, because it can also be that the tetrode was located further down and just went through the slice. This would explain why there is no canal visible within the hippocampus. Hence this is conform to the calculated positions, -5.0 mm to -5.5 mm dorsal-ventral (depending on the tetrode) and therefore below the hippocampus.

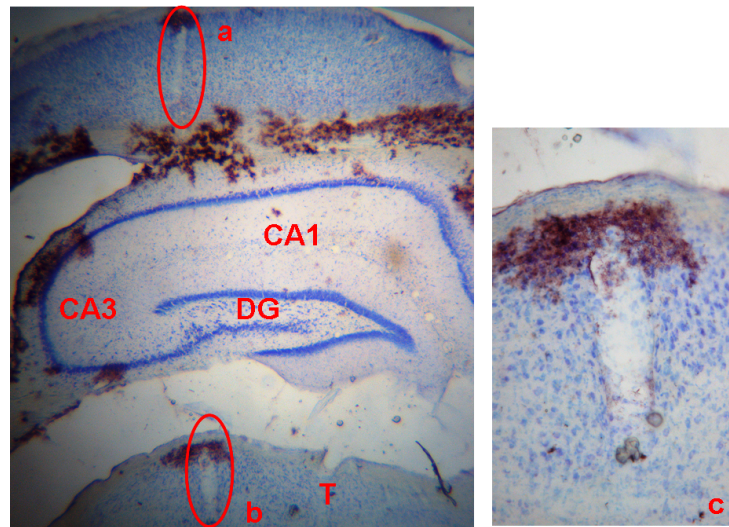


Figure 2.14: Results from the brain section T: thalamus, DG: dentate gyrus a) A 2500% enlargement shows the position of the tetrodes. As can be seen, the tetrodes were below the hippocampus c) zoom view (100x) of a) d) zoom view(100x) of b)

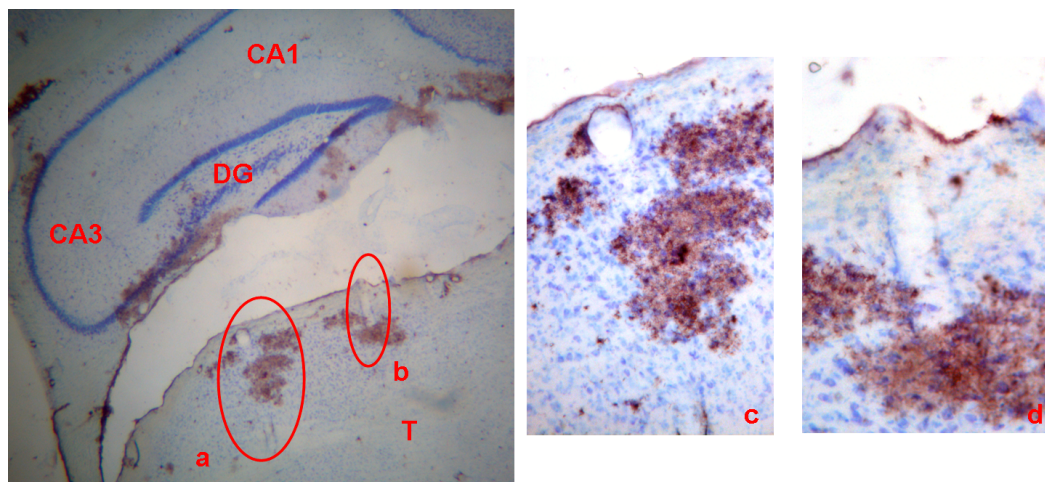


Figure 2.15: Results from the brain section(2500% magnification) T: thalamus, DG: dentate gyrus a) entrance of the tetrode b) position of the tetrode c) zoom (100x) on b

Chapter 3

Experiment 1: The Virtual Circular Road

3.1 Motivation

The motivation for this experiment is described in chapter 1.1. A circular road was chosen for the following reasons:

1. Simulating corners or walls is difficult in a virtual environment because of the missing sensory inputs. This can be avoided in taking a circular arena.
2. Since the behavior of place cells in large environments are of interest, the inner part of the circular arena can be ignored

3.2 Materials and Methods

3.2.1 The Virtual Environment

The virtual environment displayed a square of 40 m by 40 m in size. The square was enclosed by four walls each 0.6 m in height. Each wall was textured in a different pattern to provide the rats with global directional information. In the middle of the square a checkerboard-textured circular road 1 m in width and with a diameter of 20 m was placed. This road was defined as the silent

zone, which means that whenever the rat left this road, an aversive noise was played. In order to make the silent zone easier to find for the animals, a second image of the road was placed 0.5 m above the animals' headspace. To avoid a collision of the animals with the objects, they were placed at a height of 30 cm. These objects were to serve as landmarks and to provide additional global directional information to the rats. They differed in shape, pattern and number to make them easily distinguishable.

Figure 3.1 shows the environment from a side view. Figure 3.2 displays a top view.

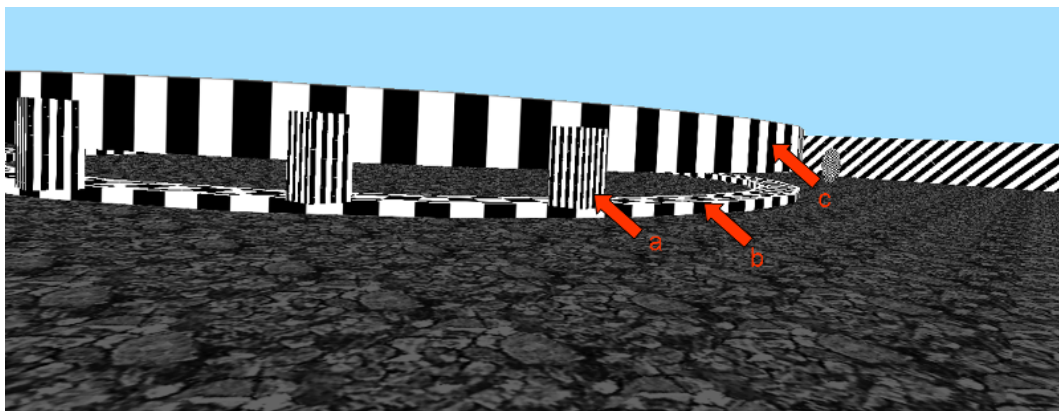


Figure 3.1: Virtual circular road a) landmark b) silent zone (road) c) guiding road

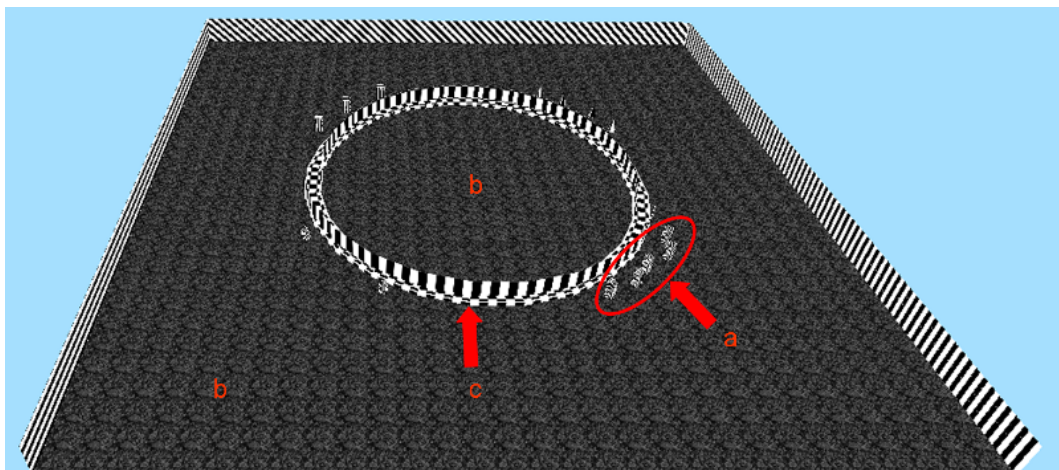


Figure 3.2: Virtual circular road a) Group of landmarks b) noisy zone c) circuit road with guiding road (silent zone)

3.2.2 The Tracking System

The tracking of the animal's position was done by the control computer. See chapter 2 Materials and Methods for details.

3.2.3 The Experimental Room

Figure 3.3 shows the layout of the experimental room. The size of the room was 3m by 4.1m. The virtual environment setup was positioned in the middle of the second half of the room. The preamplifier was placed on a rack hanging from the ceiling in the middle of the first half of the room. The control computer for the virtual environment was placed on a table close to the entrance of the room. The four speakers were positioned at 90° angles in a distance of 1.3 m around the treadmill so that the treadmill was in the center of the four speakers. To avoid turbulences of the airstream a settling chamber was used to connect two pipes with different diameters. A black curtain was hung around the virtual reality setup to hide the walls of the room.

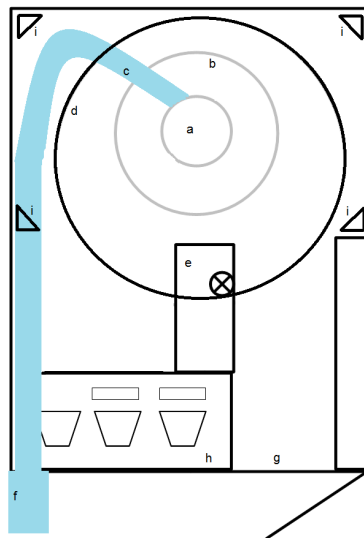


Figure 3.3: Layout of experimental Room a) treadmill b) toroidal screen c) air stream d) black curtain e) rack with preamplifier f) settling chamber g) door h) table with PCs i) speakers

3.2.4 Procedure

The animals were brought into the experimental room in their home cage. They had been water deprived for 2-4 hours. They were then put on the treadmill and attached to the angular increment counter. Then the toroidal screen was lowered into the right position and the session commenced by projecting the virtual reality. As soon as the rat would leave the road, a constant white noise sounded at a volume of 80 db until the rat returned into the circle. If the rats ran through one of the virtual walls or spend more than 30 seconds within the noisy zone, the projection stopped immediately, the screen was lightened and white noise sounded for 10s. After another 10s, the control software modified the projection so that the rat was virtually placed back to the starting position on the road. For better understanding this procedure is illustrated in Figure 3.4. Each session terminated after 15 min. The lights were then turned on, the toroidal screen was lifted, the rat was removed from the treadmill and put back into its home cage.

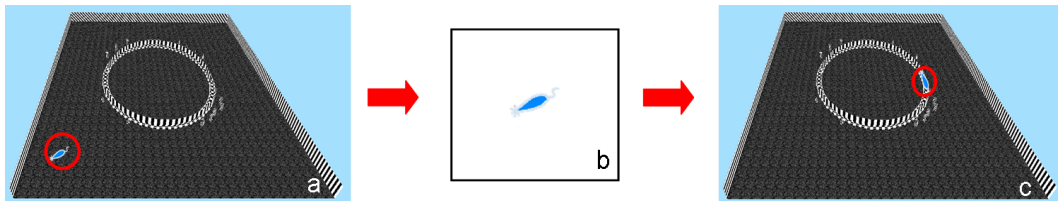


Figure 3.4: Illustration of rat running through the walls or spending more than 30s within the noisy zone a) rat runs through wall or stays more than 30 s within the noisy zone b) projection stops, screen is lightened and white noise sounds for 30 s c) rat is virtually replaced on the starting position on the road, white noise is turned off

3.3 Results

Some sample trajectories can be seen in figure 3.5. All trajectories can be found on the supplementary CD in the folder ‘Exp1_VR_trajectories’

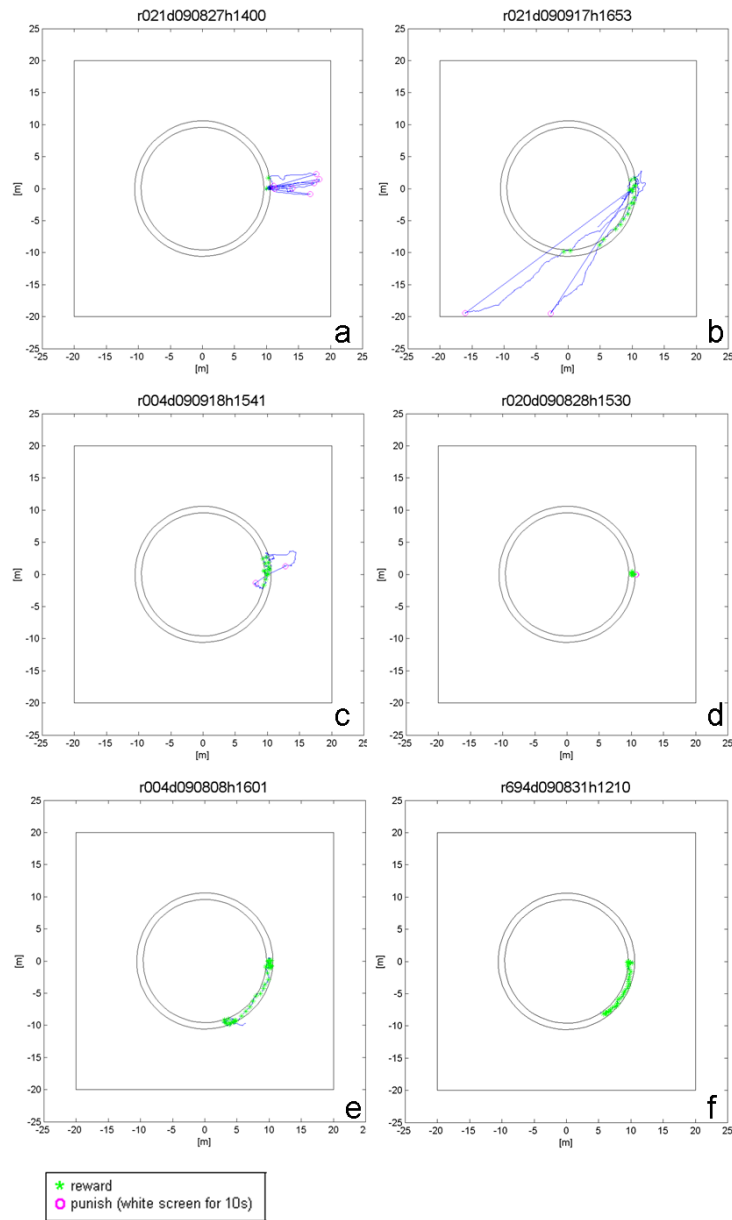


Figure 3.5: Sample trajectories

3.4 Discussion

As can be seen in figure 3.5, the performance of the rats varied extremely. While some tended to run into fixed directions (see figure 3.5 a, b), others did not move at all (figure 3.5d).

In figure 3.5 e and f two sample trajectories can be seen, where the rats followed the road. Unfortunately they were so slow, that they did not even cover $\frac{1}{4}$ of the road in 15 min. Another observation was that the rats preferred to walk right to the walls (see figure 3.5 a) or stopped walking at all as soon as they reached the noisy zone (see figure 5d). Taking these observations as input, experiment 2 ‘The Real Circular Road’ and experiment 3 ‘The Virtual Circular Arena’ were designed. This experiment was stopped before the electrophysiological recordings started.

Chapter 4

Experiment 2: The Real Circular Road

4.1 Motivation

The objective of this experiment was to teach the rats that they will be rewarded within the silent area and as soon as they enter the black area, white noise sounds and no reward will be given. Additionally this arena provides a good reference for recorded place cells and the corresponding place fields.

4.2 Materials and Methods

4.2.1 The Arena

The platform was placed on a table 0.7 m in height and consisted of two 1.2 m x 0.6 m x 0.01 m flake board plates with a white covering. The walls were made of 0.6 cm sized flakeboard of 0.6 m in height. In the middle of the platform was a white circular road with a diameter of 1.0 m and a width of 0.23 m. The dark gray circle was made of plastic with a thickness of 0.5 cm. Around the white circuit the platform was painted black (RAL 9005 Tiefschwarz). On two adverse walls the US flag and the Swiss flag were placed as landmarks each 0.21 m x 0.29 m in size. The platform is depicted in figure 4.1.

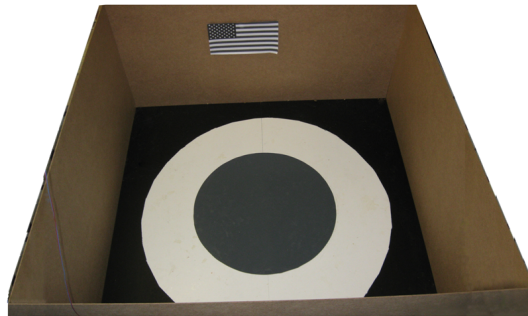


Figure 4.1: Real circular road arena

4.2.2 The Tracking System

To be able to correlate the recorded signals with the position of the animal, a small standard black and white camera was fastened on the ceiling centering the arena. Two IR-LEDs were attached to the headstage to track the position as well as the head direction of the animals. To be able to distinguish between the two IR-LEDs two different series of resistors were used. Detailed information on the system can be found in the chapter 2 Methods and Materials. Tracking was performed and processed by the hard- and software system Dacq2 (Axona, 2004a).

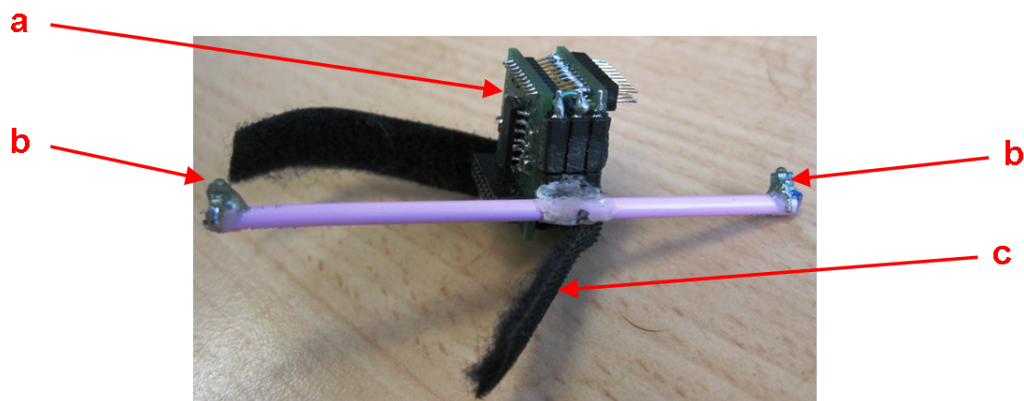


Figure 4.2: Headstage with LEDs for tracking a) circuit board b) IR-LEDs c) Velcro Tape for fastening

4.2.3 The Experimental Room

Figure 8 shows the layout of the experimental room. The size of the room was 3m x 4.1m. The real arena was placed in the middle left side of the room. The virtual environment setup was positioned in the middle of the second half of the room. The preamplifier and a light were placed on a rack hanging from the ceiling in the middle of the first half of the room. The computer for the electrophysiological recording and the control computer for the virtual environment were placed on a table in the beginning of the room. Initially the four speakers were positioned at 90° angles at a distance of 1.3 m around the treadmill so that the treadmill was in the center of the four speakers. Unfortunately when starting the first electrophysiological sessions in the virtual reality setup, the white noise showed inference with the electrophysiological recordings. In order to reduce the inference two piezo-speakers were positioned in 180° angles next to the treadmill.

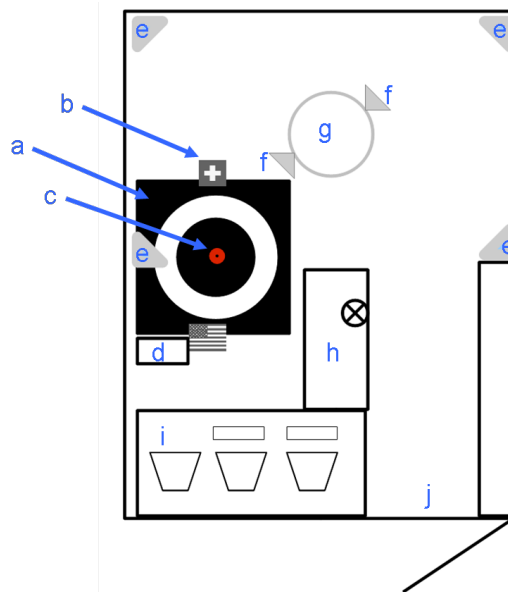


Figure 4.3: Experimental Room a) real circular road arena b) landmarks c) camera d) macrolon cage type II L e) electromagnetic speakers f) piezo-speakers g) treadmill h) rack with preamplifier and light i) table with PCs j) door

4.2.4 Procedure

Prior to testing, the animals were brought into the experimental room in their home cage. They were then put in a macrolon cage Type II L (Ehret Lab) and placed next to the arena and the experimenter. Then the headstage was attached and the recording software Dacq2 adjusted. Theta rhythm was checked and documented. For rewards little pieces of apple were spread on the circular road in the arena. After adjusting the software, lights were turned off and the animal in the cage was placed on the road in the arena. After calibrating the tracking system, the animal was released from the cage, the cage was removed and the recording system was started. Each session lasted 10 min. As soon as the animal's head was in the black part of the arena, a white noise sounded constantly at a volume of 80 db until the animal returned to the road. Since observations showed that the rats started foraging in the noisy zone when all apples were eaten, apples were refilled during the experiment in order to continue rewarding the animals for staying within the silent zone. After 10 min the lights were turned on and the animal was picked up and put back into the macrolon cage. The headstage was removed and the animal was placed back into its home cage. The analysis of the recorded data was done using TINT (Axona, 2004b).

4.3 Noise as Additional Cue

4.3.1 Results

One objective of this experiment was to test whether white noise helps to keep the animals within a certain zone. Figure 4.4 shows some sample trajectories. All trajectories can be found on the supplemental-CD in the Folder: 'Exp2_trajectories'.

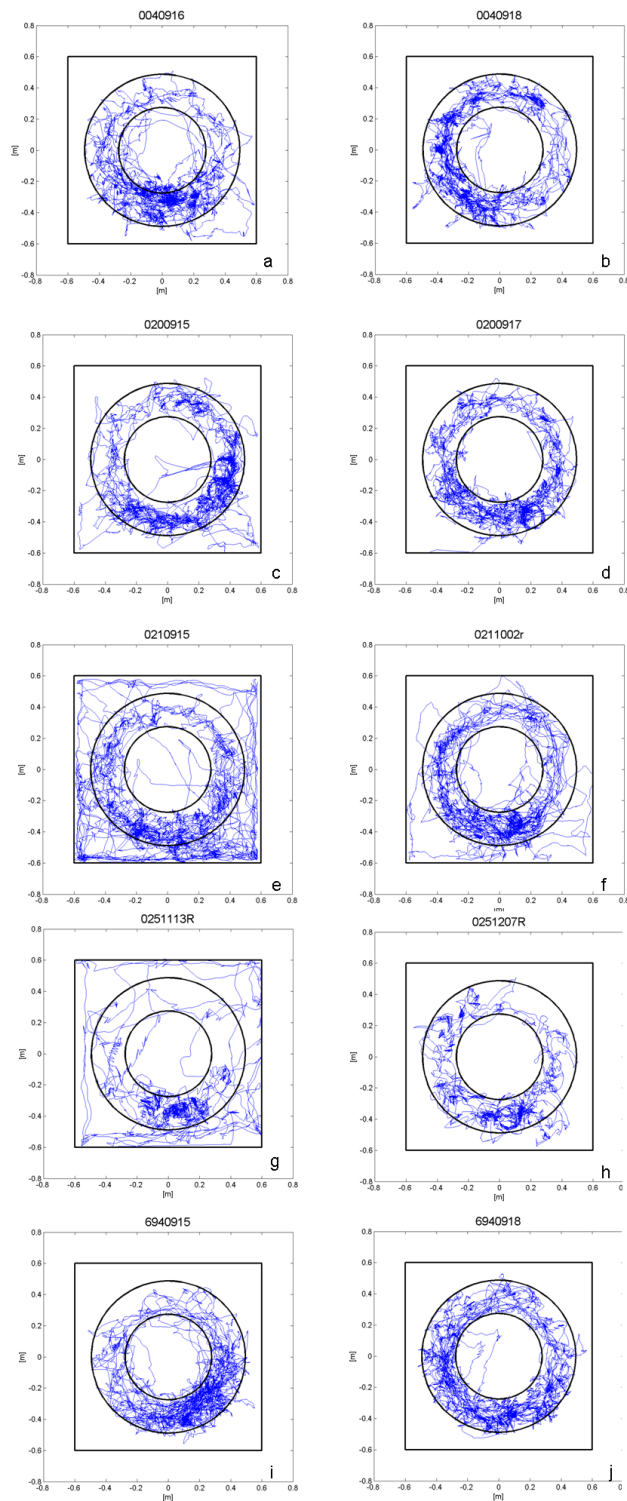


Figure 4.4: Sample trajectories from each rat a) trail 1, rat 004 b) trail 3, rat 004 c) trail 2, rat 020 d) trail 4, rat 020 e) trail 1, rat 021 f) trail 5, rat 021 g) trail 1, rat 025 h) trail 6, rat 025 i) trail 1, rat 694 j) trail 3, rat 694

A statistical analysis was performed to investigate if the noise affected the rats' sojourn time in the silent zone of the arena. The following data was collected and analyzed.

- t_{in} - the time the rat spend within the silent zone
- t_{out} - the time the rat spend within the noisy zone
- d_{in} - the distance the rat ran within the silent zone
- d_{out} - the distance the rat ran within the noisy zone

First, for comparison, time and distance were normalized by dividing them by the size of the corresponding zone A_{out} or A_{in} resulting in $t_{N(in)}$, $t_{N(out)}$ and $d_{N(in)}$, $d_{N(out)}$ (see figure 4.5 and 4.6).

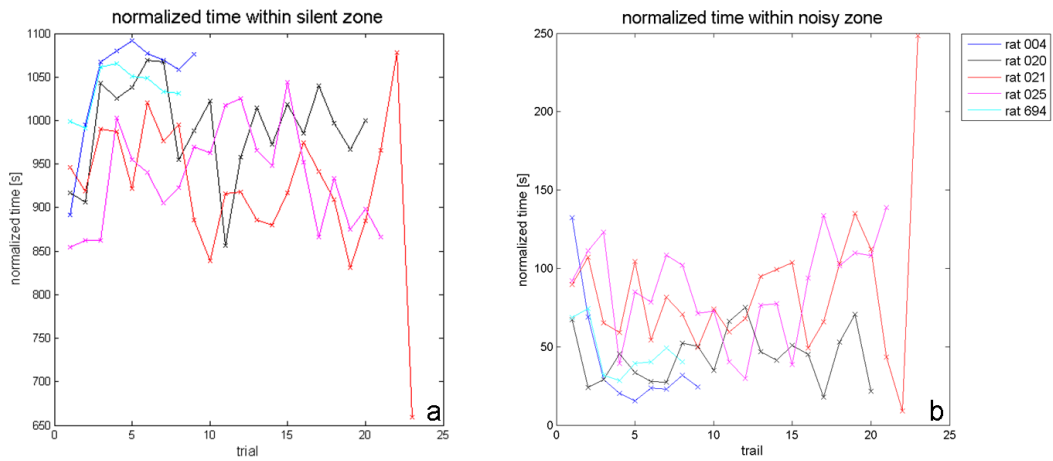


Figure 4.5: Normalized time the rats spent within the different zones.
a) silent zone b) noisy zone

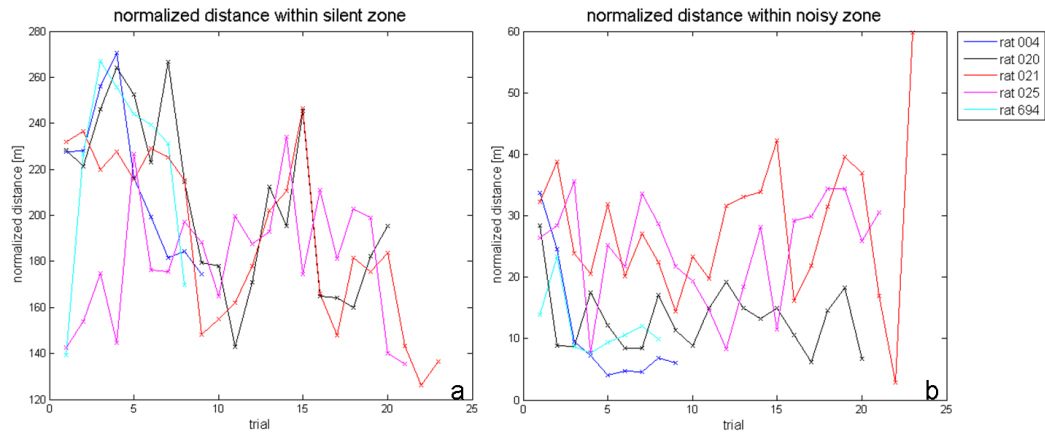


Figure 4.6: Normalized distance the rats covered in the different zones
 a) silent zone b) noisy zone

Then the average velocity v_{in} and v_{out} of the rat’s movement within the silent and the noisy zone was computed by taking the quotient of $\frac{d_{in}}{t_{in}}$, $\frac{d_{out}}{t_{out}}$ respectively.

A one-sided paired t-test with the null-hypothesis of $t_{N(out)} \geq t_{N(in)}$ was chosen to look for significant differences between the times. The results can be seen in figure 4.7.

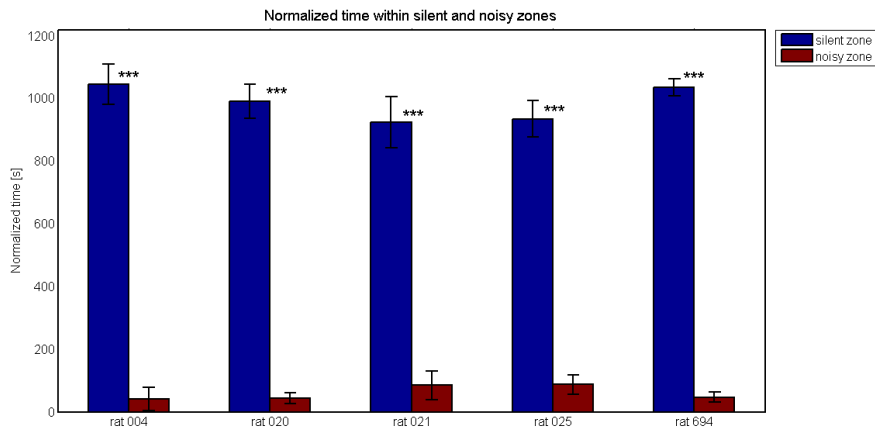


Figure 4.7: Mean and standard deviation of $t_{N(in)}$ and $t_{N(out)}$
 ‘*’: p-value<0.05, ‘**’: p-value<0.01, ‘***’: p-value<0.001

In order to get an impression of the animals’ activity, the mean distances and velocities within the different zones can be seen in figure 4.8 and 4.9. For the distances, a one-sided paired t-test with the null-hypothesis of

$d_{N(in)} \leq d_{N(out)}$ was performed. The results can be seen in figure 4.8

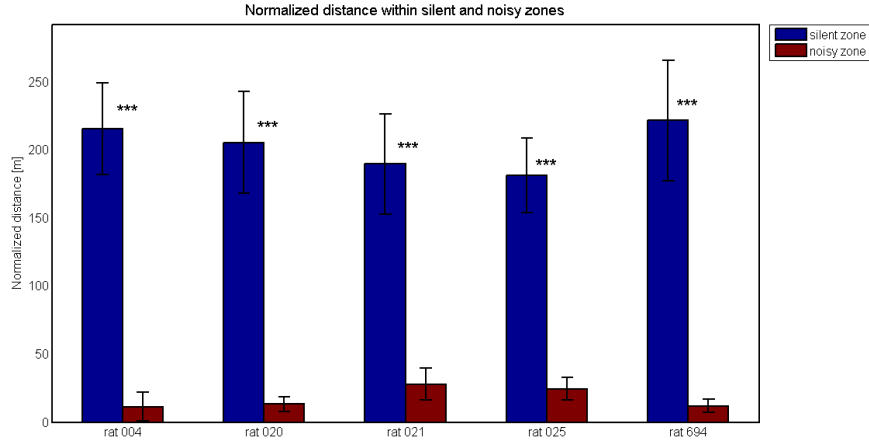


Figure 4.8: Mean and standard deviation of $d_{N(in)}$ and $d_{N(out)}$
 '**': p-value<0.05, '***': p-value<0.001

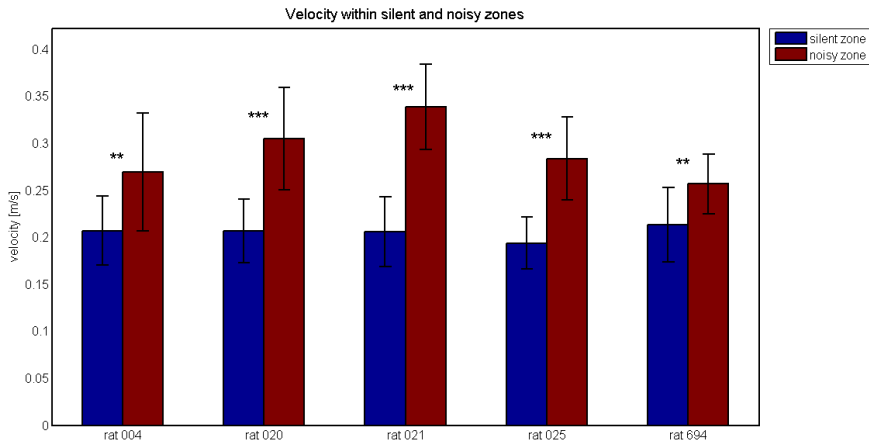


Figure 4.9: Mean and standard deviation of v_{in} and v_{out}
 '**': p-value<0.05, '***': p-value<0.001

For the differences in velocity, a one sided unpaired two-sample t-test with the null hypothesis of $v_{in} \geq v_{out}$ was performed. Results can be seen in figure 4.9. To see if the animals' behavior changed during the course of the experiment, a one-sided unpaired two-sample t-test assuming heteroscedastic variances with the null-hypothesis of $t_{in,first} \geq t_{in,last}$ was chosen. As here a comparison of the beginning and the end of the experiment was of interest, only data of the

Rat	p-value
004	0.13251
020	0.29992
021	0.72729
025	0.51602
694	0.32979

Table 4.1: Results from the one-sided two-sample t-test assuming heteroscedastic variances

first and last four sessions were taken for the test. The outcome of this test is shown in figure 4.10 and table 4.1.

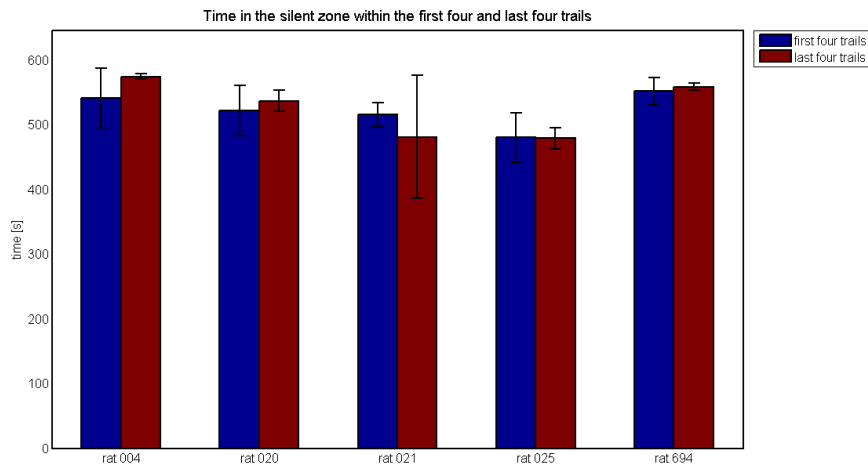


Figure 4.10: Mean and standard deviation of t_{in} during the first four and last four trails: '*': p-value<0.05, '': p-value<0.01, '***': p-value<0.001**

4.3.2 Discussion

As can be visually observed when looking at figures 4.5 and 4.7 the rats spend most of the time within the silent arena. These observations are confirmed by t-test results (see also figure 4.7). The rats also covered longer distances within the silent zone (figure 4.8). Figure 4.9 shows that the rats locomoted significantly faster within the noisy zone. The initial interpretation would be that the rats disliked the noise and therefore started running to get away from it. On the other hand the rats could have been slower (on average) within

the silent zone because they were looking for the apple pieces and spend time sitting at one point and eating them. This however would not explain the significantly larger distances the rats covered within the silent zone. The observations during the experiments showed that the rats often made very fast head movements back into the silent zone when the white noise occurred. This explains why the rats were significantly faster within the noisy zone than the silent zone without covering more distance.

Regarding the results of the t-test comparing the time within the two zones during the first and last four trails they show no significant difference. When looking at the normalized time within the silent zone (figure 4.5 a) and at the trajectories (figure 4.4) it is quite obvious that the time the rats spent within the silent area increased over the first three or four trails and then stayed at a certain level. The extreme increase of time the rats spent in the silent zone during the first four trails results in a high standard deviation and a mean value that does not differ much from the mean value of the last four trails. This of course explains the missing significance.

Putting this all together this experiment gives evidence that the white noise prevents the rats from leaving the white circle. Jan Hirschmann states in his master thesis (Hirschmann, 2009), that some rats get adapted to the white noise and start foraging into the noisy zone. Regarding the data at figure 4.10 and the t-test results these observations can not be confirmed. Most likely the rats were encouraged to move into the noisy zone when foraging for food as oatmeal was distributed throughout the whole arena. In this experiment food was only placed in the silent zone therefore no reason existed to enter the noisy zone.

4.4 Electrophysiology

4.4.1 Results

Non-place-specific Cells

During the experiments a total of seven non-place-specific cells were isolated. To ensure that the cells were not contaminated with noise or other cells, au-

tocorrelations were computed for a range of 50 ms. To see possible periodic firing behavior the autocorrelation was also computed for each cell in a range of 1000 ms.

For rat 004 two non-place-specific cells were recorded. One was stable over two recording sessions. This is shown in figure 4.11 and 4.12.

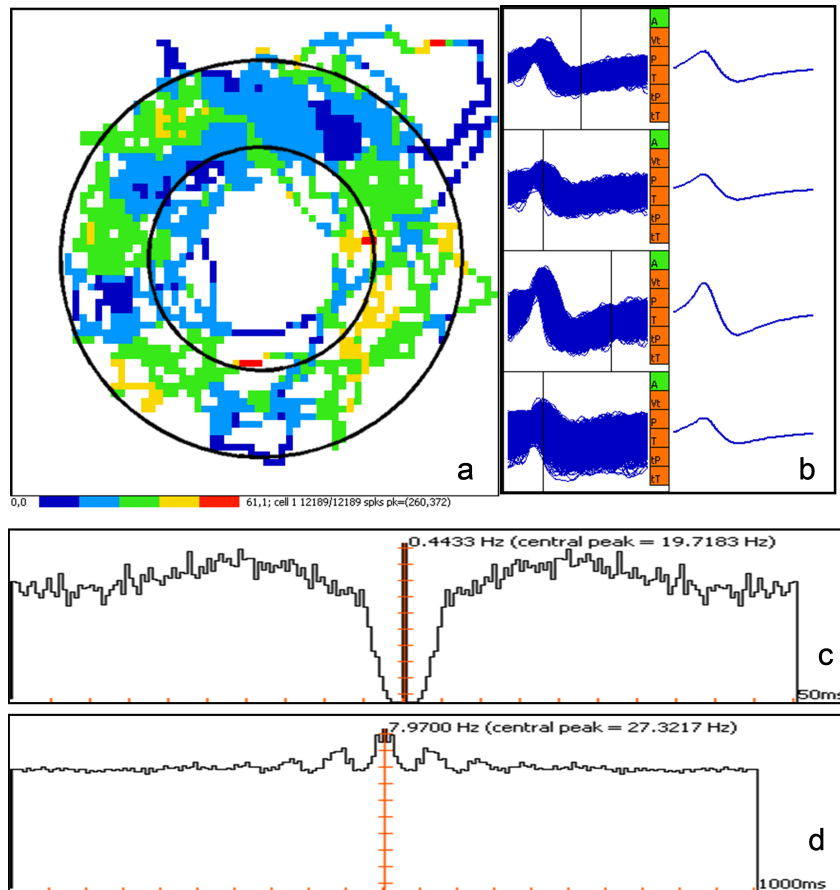


Figure 4.11: Non-place-specific cell recorded from rat 004 on September 16th, 2009 on tetrode 4 a) Density map showing the normalized firing activity of the cell. The activity was divided into five groups ([blue] 0-20% of max. firing rate, [light blue] 21-40% max. firing rate, [green] 41-60% of max. firing rate, [yellow] 61-80% of max. firing rate [red] 81%-100% of max. firing rate. The maximum firing rate of this cell was 61.1 Hz. b) summarized spikes on each tetrode (left) and the average spike shape on the right. c) autocorrelation with a time window of 50ms to show that the cell is not contaminated with other cells d) autocorrelation with a time window of 1000 ms to see periodic firing behavior

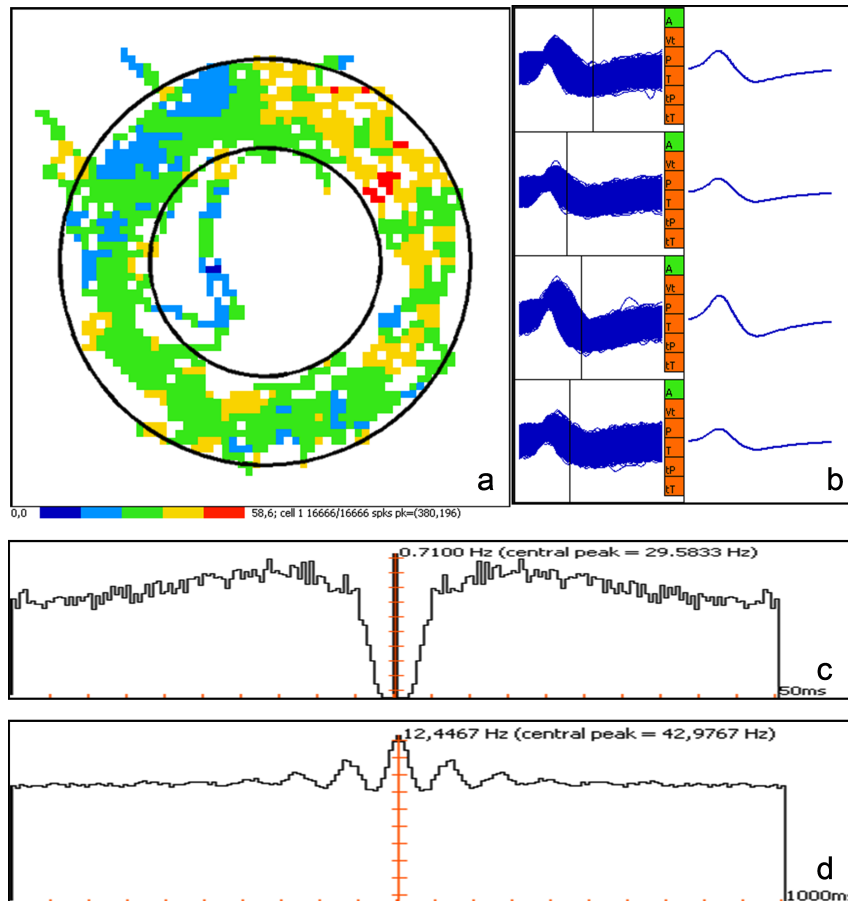


Figure 4.12: Non-place-specific cell recorded from rat 004 on September 18th, 2009 on tetrode 4 a) Density map showing the normalized firing activity of the cell. The activity was divided into five groups For description see figure 4.11. The maximum firing rate of this cell was 58.6 Hz. b) summarized spikes on each tetrode (left) and the average spike shape on the right. c) autocorrelation with a time window of 50ms to show that the cell is not contaminated with other cells d) autocorrelation with a time window of 1000 ms to see periodic firing behavior

For rat 694 two non-place-specific cells were recorded. One was stable over two days. Since they behaved similar to those from rat 004, the pictures are not shown. For rat 021 one non-place-specific cell was recorded (see figure 4.13). On the same day also a place cell was recorded on the same tetrode in the virtual environment.

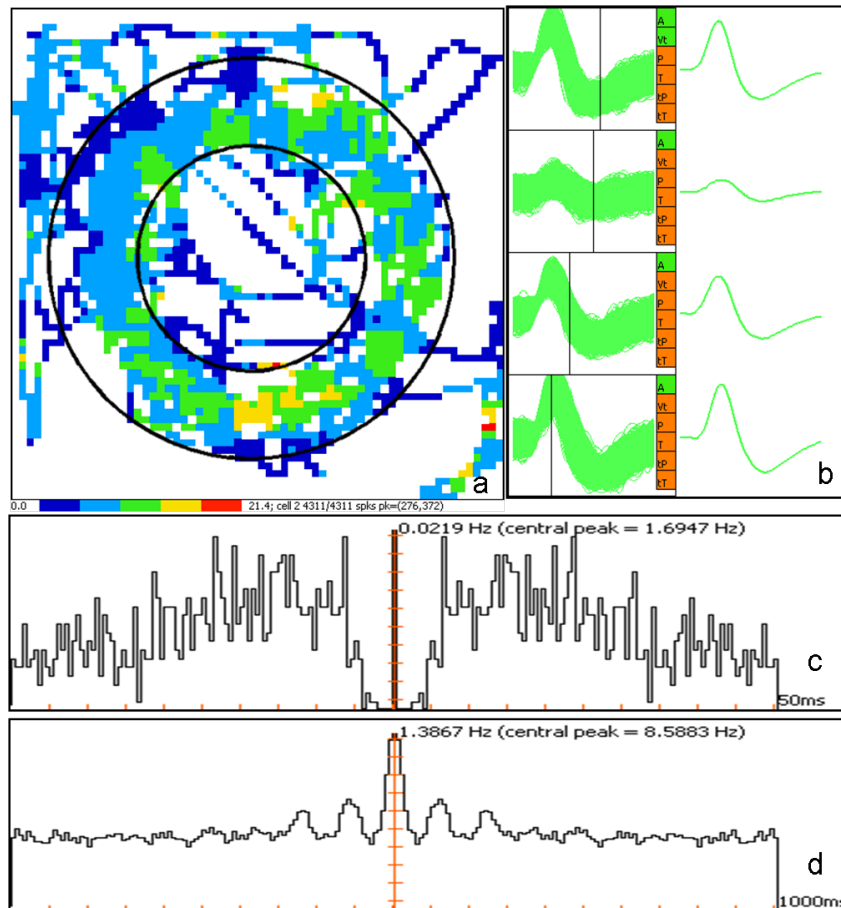


Figure 4.13: Non-place-specific cell recorded from rat 021 on January 7th, 2010 on tetrode 3 a) Density map showing the normalized firing activity of the cell. The activity was divided into five groups For description see figure 4.11. The maximum firing rate of this cell was 21.4 Hz. b) summarized spikes on each tetrode (left) and the average spike shape on the right. c) autocorrelation with a time window of 50ms to show that the cell is not contaminated with other cells d) autocorrelation with a time window of 1000 ms

Table 4.2 gives an overview of the recorded cells:

Rat	# cells	extras
004	2	One was stable for two days
694	2	Both were stable for two days
020	1	
021	1	In VR PC on same tetrode
025	0	

Table 4.2: Overview of recorded non-place-specific cells

Place cells

During the recording sessions a total of nine place cells was recorded. Auto-correlations were computed to show that the cells were not contaminated by other cells or noise. For rat 021 a total of four place cells was recorded, two of them during preliminary experiments. One was also be recorded in the virtual environment. See figure 4.14.

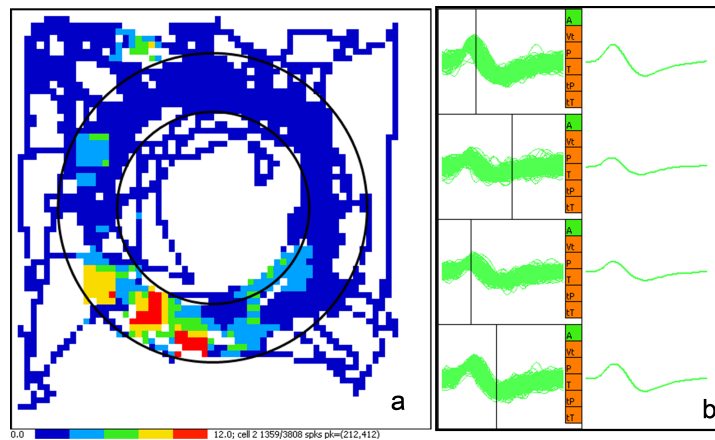


Figure 4.14: Place cell recorded from rat 021 on January 4th, 2010 on tetrode 3 a) Density map showing the normalized firing activity of the cell. The activity was divided into five groups ([blue] 0-20% of max. firing rate, [light blue] 21-40% max. firing rate, [green] 41-60% of max. firing rate, [yellow] 61-80% of max. firing rate [red] 81%-100% of max. firing rate. The maximum firing rate of this cell was 12.0 Hz. The place field is in the south-west of the circular road with a size of about 20cm x 70 cm (threshold was min 20% of max firing rate) b) summarized spikes on each tetrode (left) and the average spike shape on the right. The background firing rate was 0.633 Hz

For rat 694 two place cells were recorded. One of them was recorded over several days (see figure 4.15 and 4.16).

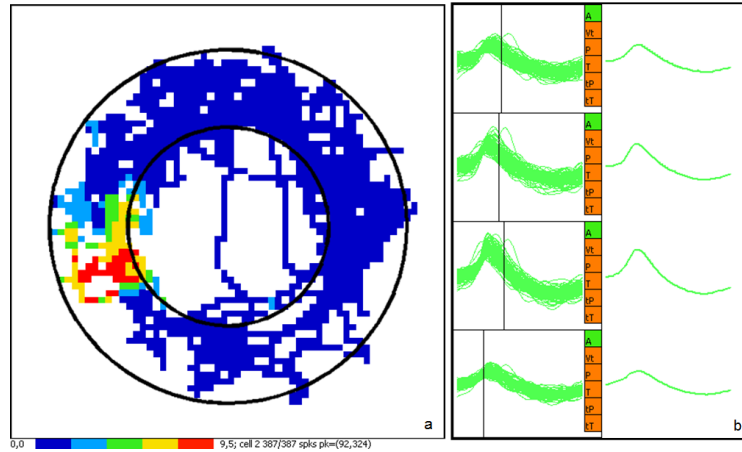


Figure 4.15: Place cell recorded from rat 694 on October 16th, 2009 on tetrode 2 a) Density map showing the normalized firing activity of the cell. The activity was divided into five groups. For details see figure 4.14. The maximum firing rate of this cell was 9.5 Hz. The place field is in the west of the circular road with a size of about 25cm x 40 cm. b) summarized spikes on each tetrode (left) and the average spike shape on the right. The background firing rate was 0.055 Hz.

Rat	# Place cells	extras
004	0	
694	1	stable for two days
020	2	
021	4	one also in VR
025	2	

Table 4.3: Overview of recorded place cells

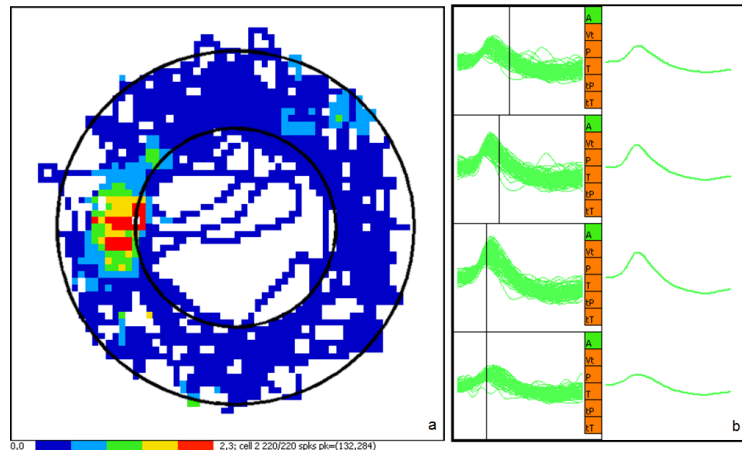


Figure 4.16: Place cell recorded from rat 694 on October 17th, 2009 on tetrode 2 a) Density map showing the normalized firing activity of the cell. The activity was divided into five groups. For details see figure 4.14. The maximum firing rate of this cell was 2.3 Hz. The place field is in the west of the circular road with a size of about 20cm x 40 cm. b) summarized spikes on each tetrode (left) and the average spike shape on the right. The background firing rate was 0.033 Hz.

4.4.2 Discussion

Non-Place-Specific Cells

Figure 4.11 and figure 4.12 show two cells recorded from the same rat same tetrode during two recording sessions within three days. Looking at the density maps it is obvious that those cells show a place-unspecific firing rate. The spike forms seem similar, channel 3 has the highest amplitude, channel 1 the second highest and channels 2 and 4 the lowest. The maximum firing rate of the cell in figure 4.11 is 61.1 Hz and for the cell in figure 4.12 it is 58.6 Hz. When comparing the size of the amplitude of channel 3 in both figures, the amplitude in figure 4.11 seems to be slightly higher.

The autocorrelations with a time window of 50 ms show clearly that the cells are not contaminated. The autocorrelation in d, show a periodic firing pattern within the fist 400 ms. The duration of 1.5 periods is about 200ms. This makes a frequency of about 7.5 Hz.

The theta rhythm in the rat hippocampus has a frequency of 4- 10 Hz (Lubenov and Siapas, 2009). In 1973 Ranck (1973) found cells in the rat hippocampus that increased their firing rate during theta irrespective of the

animals location. Due to their strong correlate to the theta rhythm he named those cells “theta-cells”. Today theta cells are known to be interneurons in the rat hippocampus. They are distinguishable from the complex-spike cells, like place cells, by having a briefer action potential and all action potentials have the same amplitude. Their firing rate lies between 10- 100 Hz.

The cells in figures 4.11 and 4.12 are by definition of Ranck (1973) theta-cells.

The cell in figure 4.13 it seems to have a non place-specific firing rate. The maximum firing rate with 21.4 Hz is quite high for a place cell. But the density map indicates clearly that this maximum is reached only in the lower east corner of the arena. In other areas the cell show a firing rate of 4.28 Hz- 8.56 Hz (light blue) and 8.56 Hz- 12.84 Hz (green) and in the lower part of the circle a maximum of 12.84 Hz-17.12 Hz (yellow). O’Keefe and Burgess (1996) report place cells having a firing rate up to 20.2 Hz. The autocorrelation in figure 4.13 c shows, that the cell is not contaminated with signals from other cells. The autocorrelation in figure 4.13 d shows a periodic firing pattern with about 7.9 Hz which is equal to the theta-rhythm. Both place cells and theta cells are known to show a correlation to the theta rhythm. But the background firing rate of 1.38 Hz indicates a place cell. Theta cells are known to have a much higher background firing rate. However this cell does not show a place specificity within this arena.

O’Keefe (Andersen et al., 2007, p.494) postulates that the size of the place field increases as one goes from the dorsal to the ventral hippocampus. And that those fields might be covering the whole arena or even larger fields. In 2005 Maurer et al. (2005) recorded from the most ventral regions of the hippocampus and found place cells with place fields twice as large as those in the middle region. Muller and Kubie (1987) reported place cells with place fields with a shape of a cylinder and a radius of 74cm. Since the arena is only 1.2 m x 1.2 m it is possible that the cell in figure 4.13 is a place cell with a place field larger than the arena itself. Especially when considering that a place cell was recorded in the virtual arena on the same day and tetrode with a place field of about 1.2 m x 0.6 m (see chapter 5.4).

Place cells

Figure 4.14 shows a place cell recorded on January 4th in rat 021. The maximum firing rate is 12.0 Hz which is within the normal range of a place cell. The action potential is broad, as expected for place cells and the background firing rate is with 0.66 Hz around 1 Hz. Interesting about this place cell is that on the same day and tetrode a place cell was recorded in the virtual environment. See chapter 5.

Figures 4.15 and 4.16 show two place cells recorded on the same tetrode on two different days. The average wave forms of both cells within the different channels are similar. The long duration of the action potential is typical for a place cell. In both recordings channel 3 has the highest amplitude followed by channel 2, 1 and 4. When comparing the amplitudes with each other those from figure 4.16 are smaller than those in figure 4.15, especially channel 4. This can explain why the maximum firing rate is significantly lower within the second recording (9.5 Hz vs. 2.3 Hz). Since the amplitude smaller during the second recording possibly the amplitude did not reach the threshold as often as before and therefor less spikes were recorded. On the other hand decreasing firing rates during different recording sessions are a well known phenomena of place cells (Andersen et al., 2007, Chapter 11).

The background firing rates of the two place cells are extremely low (0.055 Hz, 0.03 Hz). It is assumed that this is caused by the size of the clusters (387 or respective 220 spikes). Comparing the locations place fields within the two sessions it has shifted slightly upwards. Knierim et al. (1995) reported that place cells tend to have a fixed radial position within circular areas or areas with only a few visual cues. He also made the observation that the place fields may rotate within different trials. Since the arena contained only two landmarks and the rats spent most of their time within the circuit road the slight shift of the place fields is accounted to the phenomenon described by Knierim et al. (1995).

Chapter 5

Experiment 3: The Virtual Circular Arena

5.1 Motivation

As the rats showed very poor performance in chapter 3 when using a circular road, in this experiment a circular area was chosen as the silent zone. It was assumed that moving in a circular area is easier for the rats than following a road.

5.2 Materials and Methods

5.2.1 The Virtual Environment

The virtual environment displayed a square of 4 m by 4 m in size. The square was enclosed by four walls each 0.6 m in height. Each wall was textured in a different pattern to provide additional information to the rats. In the middle of the square a white flagstone patterned circle was placed with a diameter of 2 m. In order to make the white zone easier to find for the animals, a second circle was placed 0.5 m above. Flags serving as landmarks were placed on two opposing walls.

Figure 5.1 shows the environment from a side view. Figure 5.2 displays a top view. In both figures area a indicates the silent zone, area b the noisy zone.

Figure 5.1 additionally shows the two landmarks and the second circle placed 0.5 m above the first.

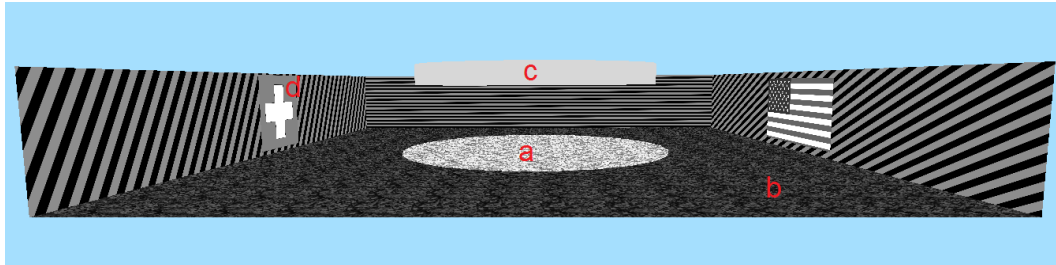


Figure 5.1: Virtual circular arena a) silent zone b) noisy zone c) second circle d) landmarks

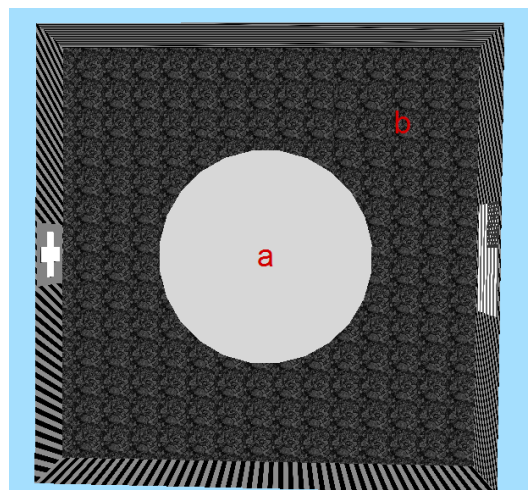


Figure 5.2: Virtual circular road a) noisy zone b) silent zone

5.2.2 The Tracking System

For tracking the position of the rats the computer used for the electro-physiological recordings was synchronized by the computer controlling the virtual reality at the beginning of each session. Synchronization tests showed that after 15 minutes there was a time difference of less than 0.01s, so further synchronization was not necessary the session. The tracking of the rat's position was done by the control computer. After the session the tracking coordinates were transferred to the position file created by the Dacq2 software (POS-File) using Matlab. For details on mapping virtual positions to camera coordinates in the Dacq2 software, see chapter 2 on Methods and Materials.

5.2.3 The Experimental Room

Figure 5.3 shows the layout of the experimental room. The size of the room was 3 m x 4.1 m. The virtual environment setup was positioned in the middle of the second half of the room. The preamplifier was placed on a rack hanging from the ceiling in the middle of the first half of the room. The computer for the electrophysiological recordings and the control computer for the virtual environment were placed on a table in the beginning of the room. As a result of experiment 2 the real arena was moved to the front of the room in order to be able to lower the toroidal screen. Originally the four speakers were positioned at 90° angles in a distance of 1.3m around the treadmill so that the treadmill was in the center of the four speakers. Unfortunately when starting the first electrophysiological sessions, the white noise showed inference with the electrophysiological recordings. This is shown in figure 5.4. To avoid turbulences a settling chamber was used to connect two pipes with different diameters. A black curtain was hung around the toroidal screen to hide the walls of the room.

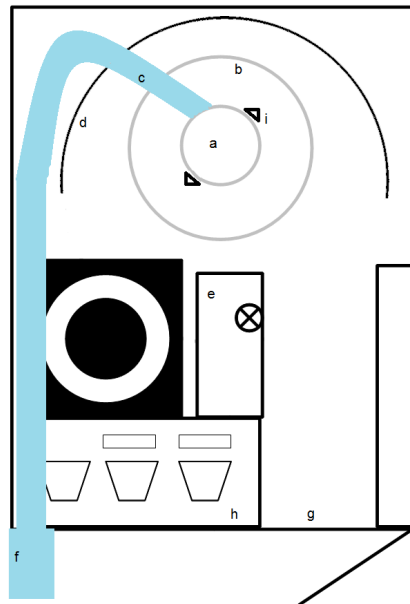


Figure 5.3: Layout of experimental Room a) Treadmill b) toroid screen c) airstream d) black curtain e) rack on the ceiling with preamplifier f) settling chamber g) door h) table with PCs i) piezo-speakers

In order to reduce the inference of the white noise, two piezo-electric speakers

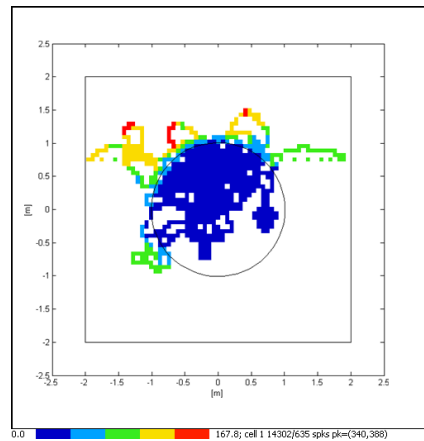


Figure 5.4: The effect of white noise on the electrophysiological recording system

were positioned next to the treadmill in a 180° degree angle.

5.2.4 Procedure

Prior to testing the animals were brought into the experimental room in their home cage. The animals had been water deprived for 2-4 hours. They were then put on the treadmill and attached to the angular increment counter. The headstage was then attached and the recording software Dacq2 was adjusted. After adjusting lights were turned off, the toroidal screen was lowered into the right position and the session commenced by projecting the virtual reality. Each session lasted 15 min. As soon as the rat would leave the white circle, a constant white noise sounded at a volume of 80 db until the rat returned into the circle. If the rat ran through the walls, the projection stopped immediately and white noise sounded for 10 s. After another 10 s, the control software modified the projection so that the rat was virtually placed on the other side of the arena within 0.2 m distance from the wall (see figure 5.5). After 15 min the lights were turned on, the toroidal screen was lifted, the animal was removed from the treadmill and put back in its home cage.

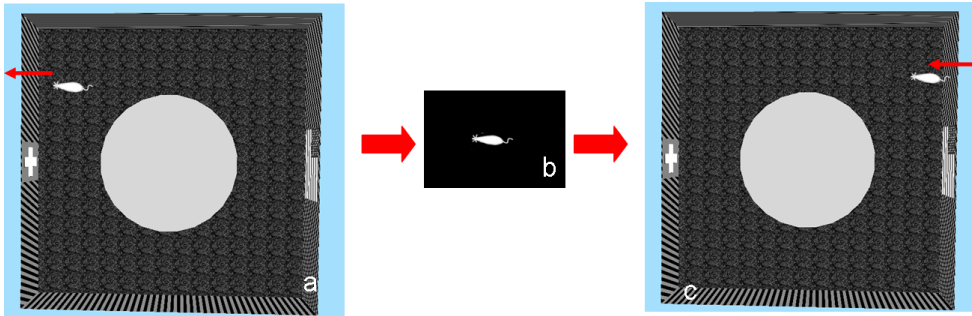


Figure 5.5: Illustration of rat running through the walls a) rat runs through wall b) projection stops and white noise sounds for 10 s c) rat is virtually replaced the other side of the arena with 0.2 m distance to the wall, white noise continues until the rat enters the silent zone

5.3 Noise as Additional Cue

5.3.1 Results

One objective of this experiment was to test whether white noise helps to keep the animals within a certain zone. In this respect the performance among the animals and the sessions varied strongly. Figure 5.6 shows some sample trajectories. All trajectories can be found on the supplemental-CD in the folder ‘Exp3_trajectories’.

To investigate if noise influences the area the rats moved in statistical analysis was performed.

The following data was collected and analyzed.

- t_{in} - the time the rat spend within the silent zone
- t_{out} - the time the rat spend within the noisy zone
- d_{in} - the distance the rat ran within the silent zone
- d_{out} - the distance the rat ran within the noisy zone
- r_n - the number of rewards the animal received during a session

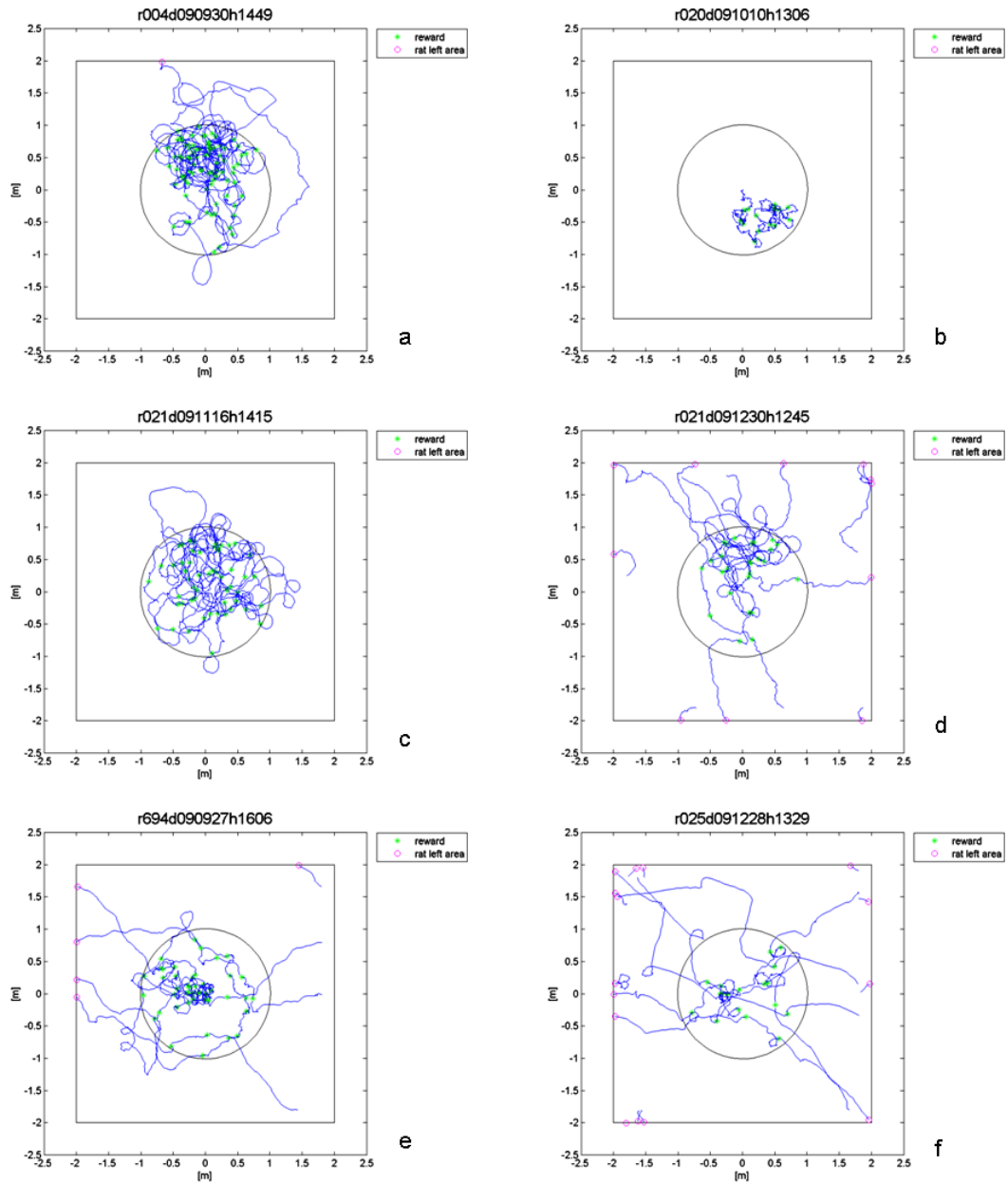


Figure 5.6: Sample trajectories from the virtual circular arena

First, for comparison, time and distance were normalized by dividing them by the size of the corresponding zone A_{out} or A_{in} resulting in $t_{N(in)}$, $t_{N(out)}$ and $d_{N(in)}$, $d_{N(out)}$ (see figure 5.7 and 5.8).

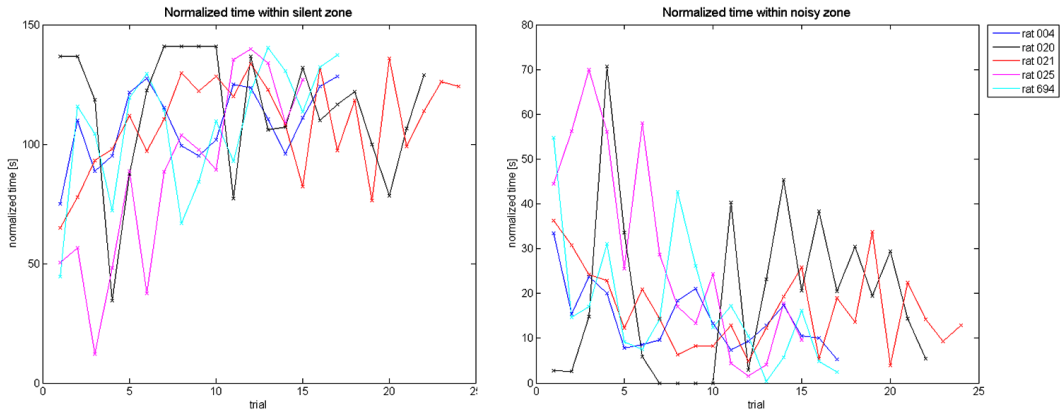


Figure 5.7: Normalized time the rats spent within the different zones.
 a) silent zone b) noisy zone

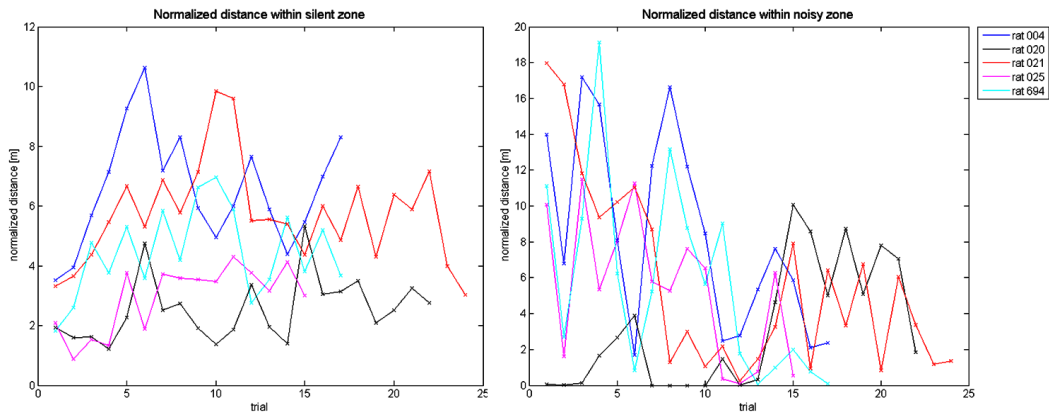


Figure 5.8: Normalized distance the rats covered in the different zones
 a) silent zone b) noisy zone

Then the average velocity v_{in} and v_{out} of the rats' movement within the silent and the noisy zone was computed by taking the quotient of $\frac{d_{in}}{t_{in}}$, respectively $\frac{d_{out}}{t_{out}}$. The reward-rate r_r was calculated by dividing r_n by $(d_{in} + d_{out})$. This is shown in figure 5.9.

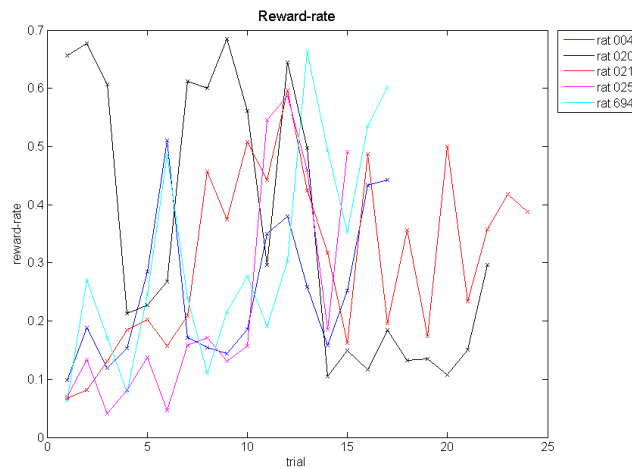


Figure 5.9: Reward-rate r_r trends over sessions

To see if there is a significant difference between $t_{N(in)}$ and $t_{N(out)}$, a paired one-sided t-test with the null-hypothesis of $t_{N(out)} \geq t_{N(in)}$ was chosen. The results of this test can be seen in figure 5.10.

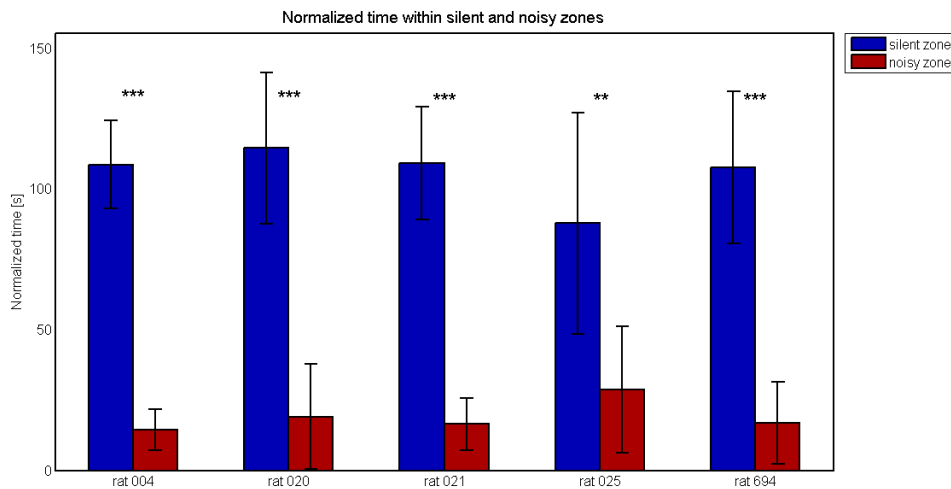


Figure 5.10: Mean and standard deviation of $t_{N(in)}$ and $t_{N(out)}$ '*': p-value<0.05, '': p-value<0.01, '***': p-value<0.001**

To compare the distances again a paired one-sided t-test with the null-hypothesis of $d_{N(in)} \geq d_{N(out)}$ was performed. For results of this test see figure 5.11.

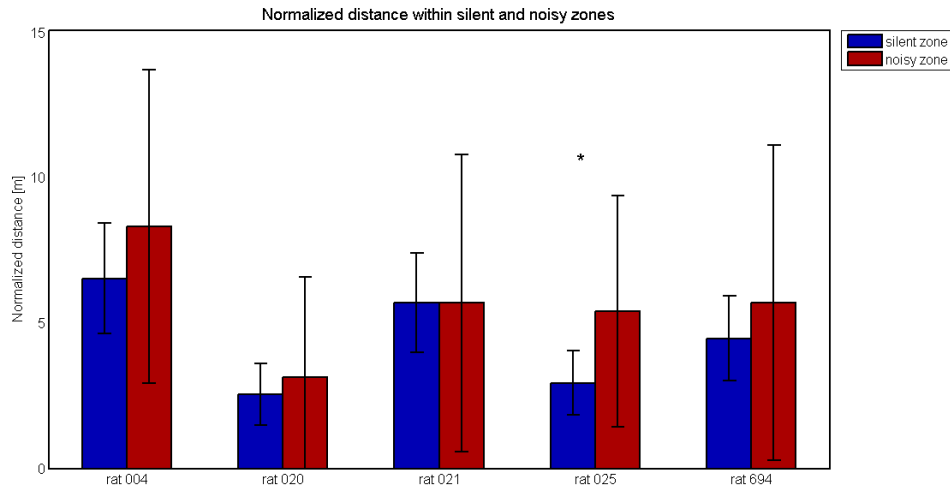


Figure 5.11: Mean and standard deviation of $d_{N(in)}$ and $d_{N(out)}$
 '*': p-value<0.05, '**': p-value<0.01, '***': p-value<0.001

Observations during the different trials suggested that the animals started to run faster as soon as the white noise sounded. Therefore a third one-sided paired t-test with a null-hypothesis of $v_{in} \geq v_{out}$ was performed. The results are shown in figure 5.12.

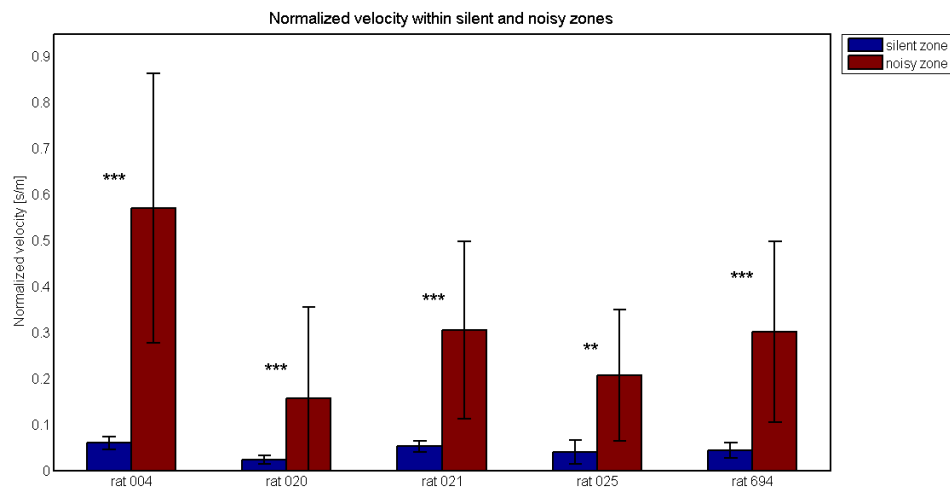


Figure 5.12: Mean and standard deviation of v_{in} and v_{out}
 '*': p-value<0.05, '**': p-value<0.01, '***': p-value<0.001

To see if the animal's behavior changed during the course of the experiment, a one-sided two sample t-test assuming heteroscedastic variances was chosen. As here a comparison of the beginning and the end of the experiment was of interest, only data of the first and last five sessions were taken for the test. The outcome of this test is shown in figure 5.13.

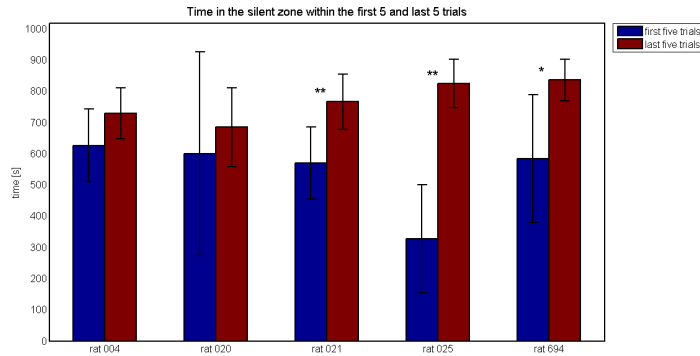


Figure 5.13: Mean and standard deviation of t_{in} during the first four and last five trials: '*': p-value<0.05, '**': p-value<0.01, '***': p-value<0.001

As can be seen from figure 5.13, the t-test was only significant for three out of five animals. Hermann Ebbinghaus, the pioneer in learning curves, setup the theory that learning has a strong growth at the beginning of the learning process and then gradually decreases until a certain level of performance is reached (Ebbinghaus, 1885). This theory implies that a regression analysis can be deployed to get a more accurate impression on how the rat's performance changed during the experiment.

For the regression analysis the ratio $d_{N(r)}$ of $d_{N(out)}$ and $d_{N(in)}$ and the ratio $t_{N(r)}$ of $t_{N(out)}$ and $t_{N(in)}$ was computed. An exponential decay curve for the $d_{N(r)}$ and the $t_{N(r)}$ is expected. The rationale for this assumption lies in the increasing time spent and the increasing distance covered by the animal in the silent zone, while at the same time the time spent and distance covered in the noisy zone decreases. This causes a decreasing ratio of $d_{N(r)}$ and $t_{N(r)}$. Since the more time respectively distance the animals spent within the silent zone, the lower the ratio would be. For the reward rate an upper bound of 1 is given, therefore a bounded exponential curve is expected. As can be seen

from figure 5.9, none of the rats ever reached a reward-rate of more than 0.7. This observation is compliant with the experiments performed by Jovalekic (2008). Here also none of the rats had a reward-rate of more than 0.87 within the observed time. Therefore when modeling the curve the upper bound of 1 was ignored.

The model curves for distance and time ratios and the reward rate are depicted in figure 5.14. As can be seen, both curves are variants of exponential curves, therefore the x-axis was log-transformed to receive a linear slope instead on an exponential one. Then a linear regression was performed.

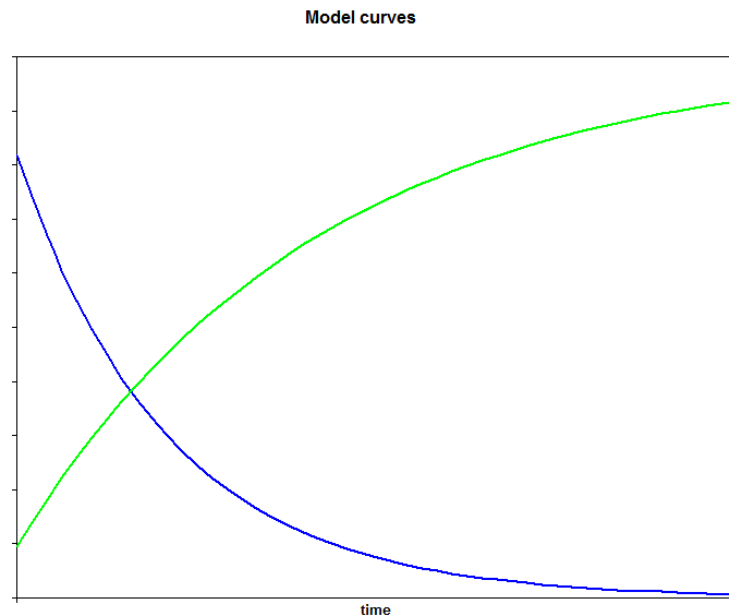


Figure 5.14: Expected curves [blue] model curve for time- and distance ratio, [green] model curve for reward-rate

Table 5.1 shows the results of the linear regression computed for the reward rate. It includes values for the computed slope, y-intersect, the confidence intervals (CI) for the slope and the p-values 1 and 2 and R^2 . The p-value 1 gives evidence on the null-hypothesis that the slope is equal to 0. R^2 shows to what extent the variance of the data can be explained by the time variable. P-value 2 is a rating for the fit of the model. All computations were done using the MATLAB built-in ‘regress’ and ‘regstats’ functions.

Table 5.2 and 5.3 show the results of the linear regression of the distance-ratio and the time-ratio. The computational variables are identical to the ones in

Rat	slope	y-intercept	CI (95%)		p-value 1	R^2	p-value 2
004	0.079	0.096	0.003	0.156	0.00863	0.246	0.04266
020	-0.512	-0.114	-0.832	-0.192	7.4617E-10	0.357	0.00320
021	0.106	0.068	0.040	0.172	0.00061	0.335	0.00307
025	0.938	-3.362	0.492	1.384	0.00174	0.661	0.00945
694	0.145	0.025	0.047	0.243	0.00278	0.400	0.00643

Table 5.1: Results from the linear regression of the reward rate P-value 1 is the p-value of a t-test with the null hypothesis that the slope is equal to zero, p-value 2 is a measure for the goodness of fit of the model

Table 5.1.

Rat	slope	y-intercept	CI (95%)		p-value 1	R^2	p-value 2
004	-0.960	3.334	-1.460	-0.460	6.46998E-09	0.527	0.00096
020	1.745	-8.085	-2.805	6.295	5.98328E-08	0.031	0.00628
021	-1.376	4.349	-1.795	-0.958	1.97621E-16	0.679	0.00000
025	-1.573	2.669	-2.663	-0.484	1.6128E-08	0.479	0.00020
694	-1.569	4.548	-2.417	-0.720	1.07852E-09	0.509	0.00131

Table 5.2: Results from the linear regression of the distance ratio ($d_{N(r)}$)

Rat	slope	y-intercept	CI (95%)		p-value 1	R^2	p-value 2
004	-0.090	0.323	-0.140	-0.040	1.34233E-08	0.498	0.00155
020	0.835	-7.149	-3.416	5.085	9.0084E-10	0.008	0.71937
021	-0.093	0.386	-0.154	-0.032	2.67285E-11	0.313	0.00451
025	-1.894	1.678	-2.683	-1.105	2.79023E-08	0.717	0.00092
694	-0.250	0.716	-0.411	-0.090	2.73128E-09	0.423	0.00469

Table 5.3: Results from the linear regression of the time ratio ($t_{N(r)}$)

5.3.2 Discussion

During the observation different strategies could be identified. While some rats tend to turn around as soon as they reached the noisy zone (see figure 5.6 c), others start to run straight ahead, pass the walls and when gotten virtually re-located on the other side of the wall, ran straight back into the silent zone, collected their reward and then left the area again (see figure 5.6 e and f). Some rats did not walk much at all and turned in small circles to

receive their reward (see figure 5.6 b).

Another observed behavior was that some rats tended to walk straight through the wall after having been virtually “re-located” (see. Figure 5.6 d, f) and then started licking at the reward tube. Since there was still white noise one can assume that the rats did not learn that reward is only given within the silent area. Unfortunately every time the rats ran through the wall a bell rang, but this also happened when the rats received a reward. Although the two sounds were different, they were possibly not different enough to be distinguishable by the rats. As soon as this behavior was detected the ringing when leaving the area was turned off. Unfortunately this was within the last days of the experiments so not enough data could be collected to see if this was one of the reasons the rats went through the walls that often.

In some trials the rats turned so often which twisted the reward tube until it got blocked. In some cases this caused the rats to enter the noisy zone and run through the walls. Although after observing this behavior the reward tube was twisted in the other direction before the trial (which was counterclockwise in all cases) this event could not always be prevented.

Looking at the t-test results for the $t_{N(in)}$ vs. $t_{N(out)}$ it is obvious that the paradigm worked and the animals did spend significantly more time within the silent zone. Although the p-value for the distance (silent) vs. distance (noisy) is not significant except for rat 025, this can be easily explained by the results of the velocity t-test. The animals started running when the white noise occurred and therefore covered more distance in less time than in the silent zone. These results confirm the impressions during the observations.

Taking the results of the one-sided unpaired t-test comparing the time the rats spend within the silent zone during the first five and the last five trials only rat 021, 025 and 694 had significant changes. As expected all rats (except rat 020) showed a significant positive slope for the reward rate and a negative slope for the distance-ratio and time-ratio in the linear regression results. These results confirm the assumed learning curve. All p-values are < 0.05 indicating that the R^2 is sufficiently high and therefore the model fits for the data. Whether this finding can be accounted for by the white noise or the reward the rats received within the silent zone, or both can't be said. But

this is not the question of this thesis. Here noise was only used as additional cue to keep the rats within an area. It was not to be investigated if this was the only cue.

One can assume that rat 020 spent increasing time within the noisy zone over the different trials. The figures 5.7 and 5.8 show that during the first three trials and during trial 7-9 rat 020 spent the complete session time within the silent zone. Looking at the overall distance within the silent zone it is clear that rat 020 did not move at all during those trials and therefore had a very low probability to enter the noisy area by chance. One sample trajectory from rat 020 during those trials can be seen in figure 5.6 b.

When rat 020 started to become more active it also started leaving the silent zone and therefore was able to learn the paradigm.

The same reason might explain why rat 020 is the only rat which has a positive slope in the regression analysis for the reward-rate. During trials 1-3 and trials 7-9 rat 020 turned around his own axis (see figure 5.6 b for an example trial and figure 5.8 for distances). That is why the reward rate is only ca. 0.7 during these trials. One would expect the reward rate to be 1 if the animal stays within the silent zone all the time. The distance for the reward rate was computed by taking the distance the animal covered multiplied by the sinus of the angle the animal running in. This ensured that the rats had to cover real distance to get the reward and could not turn in small circles. So in case of rat 020 the linear regression model did not fit as shown by the p-value 2 in table 5.3.

The rat was simply not active enough to get sufficient experience allow the rat to learn the paradigm.

This problem can be avoided, when control trials were done without noise. But due to time limits and the fact that the main focus was on the electrophysiology and not the influence of the white noise on the rats behavior no control trials were done. Additionally one has to mention that when first doing the control trials and then the conditioned trials, the rats would get more experience in maneuvering in the virtual environment and therefore might have a different initial state during the control and conditioned experiments. Running the control and conditioned experiments on the same time (e.g. same day) would not help either because the rats never know if the noise occurs

when they leave the with zone or not and therefore might behave differently, than if the have no experience with noise in the black colored area.

The approach using noise as an additional cue was a full success. However to get more significant results more experiments are needed.

5.4 Electrophysiology

5.4.1 Results

During the experiments in the virtual environment a total of two place cells was identified. These can be seen in figure 5.15 and figure 5.16.

Auto-correlation was computed for each cell to show that the cell is not contaminated. No spikes were found during the refractory period.

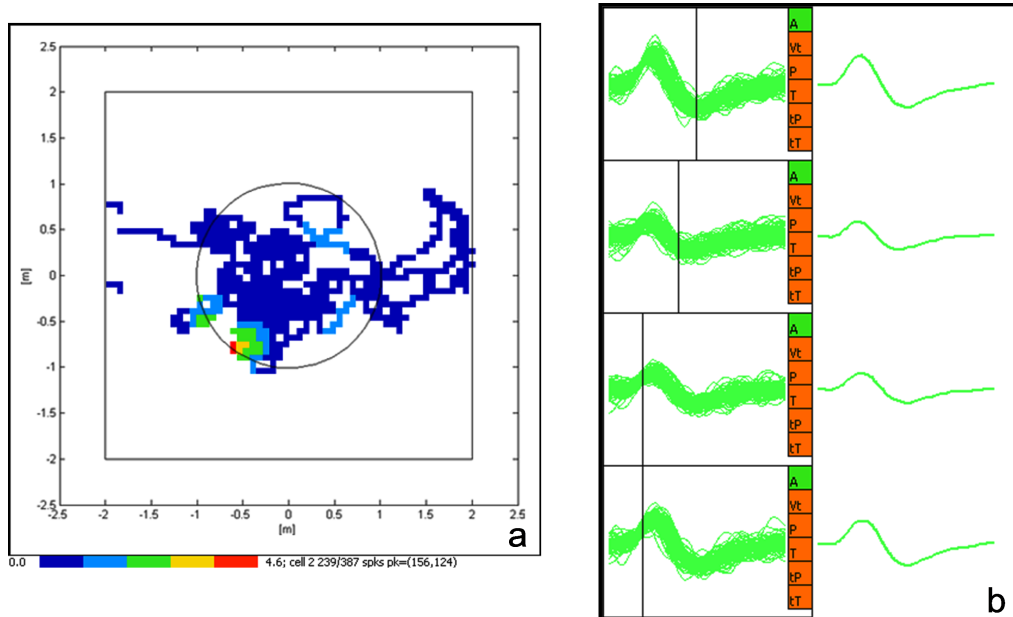


Figure 5.15: Place cell recorded from rat 021 on January 4th, 2010 on tetrode 3 The activity was divided into five groups. ([blue] 0-20% of max. firing rate, [light blue] 21-40% max. firing rate, [green] 41-60% of max. firing rate, [yellow] 61-80% of max. firing rate [red] 81%-100% of max. firing rate. The maximum firing rate of the cell was 4.6 Hz. The place field is in the lower left part of the circle arena. On the same day and same tetrode, another place cell was identified in the real arena (see chapter 4.3.2.). The size of the place field is, assuming the form of an eclipse and taking a threshold of 20% of the maximum firing rate) 1m x 0.6 m b) shows the sum of the spike waves (left) and average (right) as recorded on each tetrode. The background firing rate was 0.0321 Hz

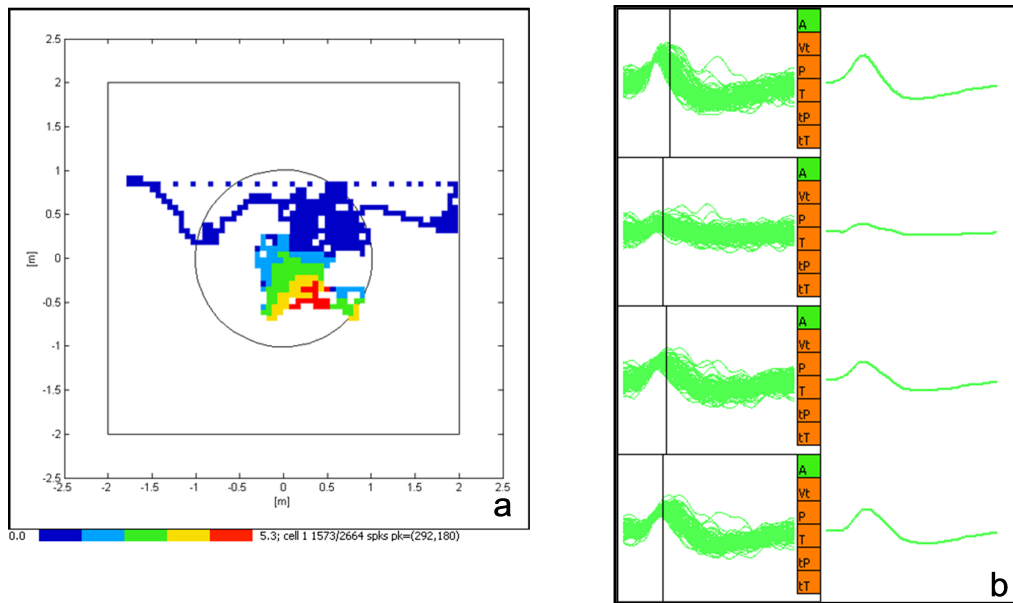


Figure 5.16: Place cell recorded from rat 021 on January 7th, 2010 on tetrode 3 a) Density map showing the normalized firing activity of the cell. b) shows the sum of the spike waves (left) and average (right) as recorded on each tetrode. A scaling of five was used to describe the intensity of activity, see figure 5.15 for details. The maximum firing rate of this cell was 5.3 Hz. The place field is in the middle to right part of the circle arena. On the same day and same tetrode, another cell was identified in the real arena (see chapter 4.3.2.), without being place-specific. The size of the place field is, assuming the form of an eclipse and a minimum of 20% of the max firing rate, 1,5m x 1.1 m. The background firing rate of this cell was 0.1117 Hz

5.4.2 Discussion

As can be seen in the results section two place cells were isolated. Both cells recorded on the same rat and same tetrode. Since the tetrode was lowered between the trials for about $100\mu\text{m}$ it is very unlikely that the recordings show the same cell.

Due to the poor performance of the rat the size of the place fields could only be estimated. With 1 m x 0.6 m and 1.1 m x 1.5 m the size of the place field seem large. But according to Jung et al. (1994) the size of the place fields increases to the ventral of the hippocampus. The position of the tetrodes were -2.5 mm dorsal-ventral and - 2.6 mm , which is at the ventral site of the hippocampus. As the isolated cells were not stable over more than one session and therefore the basic experiments with rotation of the landmarks or changing the size of the area could not be performed.

For a comparative discussion of the results from experiment 2 and 3 see chapter 6.2 general discussion.

Chapter 6

Discussion

6.1 Comparison of the Microdrive Architectures

Two different types of microdrives were used in the experiments. The ones purchased from Axona required less effort to assemble. Attaching the tetrodes took less than a day; coating the connections with nail polish and platinizing the tetrodes approximately two days.

The construction of the self-made microdrives took 2-3 full days and needed much more fine motor skills.

When recording the rat having the Axona microdrive with the Axona male connector implanted, the white noise produced more inference than when recording from the other rats. But since tests with the testing generator showed that the increase of inference was caused by the headstage and not the microdrive this can be avoided by using the Axona microdrive with a precision male connector.

Unfortunately not enough place-cells could be recorded to determine which microdrive architecture leads to more stable place fields. Here more experimental work is needed.

6.2 Electrophysiology

Place cells in both the real and virtual arena could be identified. Although the number of recorded place cells within the real arena is higher than within the virtual arena it must be pointed out that four of the place cells recorded in the real arena were identified during preliminary experiments or during sessions in experiment 2 where no recording took place in the virtual environment. Although the tetrodes were not moved prior to recordings in the virtual reality setup, the cells were lost before the recordings in the VR started.

On January 4th, 2010 on the same tetrode in both environments a place cell was identified in rat 021. In the real environment the place field was in the south west of the circular road and the size was approximately 20 cm by 70 cm. The maximum firing rate was 12.0 Hz. In the virtual environment the place field was localized in the south-west area of the silent zone. The size was approximately 1m by 0.6m and the maximum firing rate 4.6 Hz.

As has been showed by O'Keefe and Burgess (1996) the size of the place field changes with the geometry of the environment. Unfortunately the exact size of the place field could not be determined because the place field in the virtual environment was on the edge of the trajectory of the rat. It has been shown before (O'Keefe and Burgess, 1996) that the maximum firing rate varies over different recordings and environments. But when comparing the average spike form of the two cells, they are identical. Therefore it can be assumed that the recorded cell in the real environment is the same as the one in the virtual environment. This is definitely a novelty as it has not been shown in previous studies.

Being that the cell found was not stable over more than one day in both the real and the virtual arena, no further experiments like changing the position of the landmarks or the size of the environment could be done.

6.3 Comparing the performance in the real and the virtual environment

The major difference between this study and previous studies done with virtual reality setups was the use of white noise as additional cue. The idea was to keep the rats from leaving a certain area. In experiments 2 and 3 (the VR circular arena and the real circular road), the results showed that this paradigm worked and the rats learned to stay within the silent area.. The t-test results comparing the time the rats spent within the silent zone during first four and last four trials were insignificant for all animals in experiment 2. In chapter 4 it is assumed that this is due to a learning effect of the animals. As expected, after 4 trials the rats had learned the paradigm. This is confirmed by the marginal differences in the mean value. Additionally the dramatical improvement of performance during the first four trails leads to a high standard deviation. High standard deviation and mean value explains the low significance.

When comparing the results of experiment 2 with the results of experiment 3, it shows that it is easier for the rats to navigate in the real than in the virtual arena. This result is conform with the results from Hölscher et al. (2005). Here the rats learned the task within the first four sessions in the real arena while still improving their performance significantly within the first ten trails in the virtual arena.

This shows clearly that there is a strong difference in navigating in the virtual environment as is in the real environment for the animals. Definitely this can be accounted to other influencing factors such as the absence of sensory inputs like smell or touch. Also the virtual environment contains cues that are stable and possibly disturb the action-perception loop that the rat receives while moving. One of these cues is the frame holding the angular increment encoder. Others are the projector above the rat and the seams of the toroidal screen. Recently Harvey et al. (2009) published a paper where they recorded place cells in mice navigating in a virtual environment. The architecture of the virtual reality setup is based on the one used in the present study. The main difference was the fixation of the animal. The mice were head-restrained and therefore not able to turn around their own axis. In order to do this in the

virtual environment they had to twist the Styrofoam sphere. The head-fixation was necessary because Harvey et al. (2009) recorded intracellularly but fixating them also has the advantage of the stable visual cues like projector and the seams of the toroidal screen, are always in the same place and therefore might not be perceived by the mice after a certain time. This is comparable to a person wearing glasses and stops noticing the frames after a while.

According to Dr. Hansjürgen Dahmen, who was co-author of the paper published by (Hölscher et al., 2005), they tried to body-fixate a rat but soon found out that rats were not suited for this kind of experiment. They only moved in large circles and therefore did not show common trajectories anymore.

Additionally, as mentioned in chapter 1, rats have a good auditory system. Auditory cues like the controlling-computer, the TV for the observation of the animals or the experimenter most likely have a disturbing influence. In a real environment one would expect an auditory cue to change in volume depending on the distance to the cue. But when navigating in the virtual environment for example the distance of the rat to the controlling-computer always stays the same and so the volume of the noise produced by the controlling-computer neither increases nor decreases by distance.

Chapter 7

Conclusion and Outlook

As done in the two previous studies (Jovalekic, 2008; Schnee, 2008), this study clearly shows evidence that the visual stimuli presented by the virtual reality setup are sufficient enough for the place cells to develop place fields that show a firing pattern which can be correlated to a location in the virtual environment.

What this work additionally shows is that the use of auditory cues can improve the performance of the rats. White noise was used to keep the rats within a certain area and apparently prevented them from running into fixed directions. Another finding was that the willingness to move in a virtual reality setup varies extremely among the rats. Therefore it is recommended to undergo a selection process for the test animals by their ability to perform in a virtual environment. This should be performed prior to head-stage surgery.

The silent area was colored white while the noisy area was colored black. Due to the reflections caused by the screen and the large white area, the contrast was lowered and the luminance within the virtual reality setup was high when the rat was within the silent zone. As explained in chapter 1 the rats' visual system has a low acuity. However, rats are able to detect elements smaller than the acuity if the contrast is high enough. Moreover, rats show a strong preference of dark light. Considering this, an inverse design of the virtual environment where the silent zone is dark and the noisy zone is light, may lead to a better performance. This would not only combine the aversive stimuli noise and light, it would also reduce the reflection and increase the

contrast when the rat stays within the silent zone.

Another observed problem was the little distance the rats covered during the experiments. Rewards were given dependent of the distance the rat covered. Giving the rewards at certain visibly marked points in the environment, for example like the cylinders in the study of Hölscher et al. (2005) will possibly increase their motivation to move. To ensure that the rat runs through the same place several times, the cylinders could be arranged in a circle. To achieve a more 3-dimensional impression, the white noise could be increased according to the distance of the silent zone.

Altogether this study encourages further investigations of the fire activity of place cells in virtual environments. Especially some basic experiments like remapping or changing the size of the virtual environment should be done to investigate if the behavior of place cells in virtual environments is comparable to the behavior in real environments. Also it would be worthwhile investigating the influence of a constantly changing environment on the firing activity of the place cells. This can only be done in a virtual environment.

Bibliography

- Alberti, L.-B. (1435). *De Pictura*. Leon-Battista Alberti.
- Andersen, P., Morris, R., Amaral, D., Bliss, T., and O’Keefe, J., editors (2007). *The Hippocampus Book*. Oxford University Press.
- Anderson, M. and Jeffery, K. (2003). Heterogeneous modulation of place cell firing by changes in context. *J Neurosci*, 23(26):8827–8835.
- Axona (2004a). *Dacq Recording System User Guide*. Axona Ltd, St. Albans, UK, 148 Green Lane, St.Albans, Herts, AL3 6EU, 4.0 edition.
- Axona (2004b). *Tint Cluster Cutting and Analysis Software*. Axona Ltd, St. Albans, UK, 148 Green Lane, St.Albans, Herts, AL3 6EU, 4.0 edition.
- Axona (2009). *Axona MDR-XX Microdrive User Guide*. Axona Ltd., St. Albans, U.K., 148 Green Lane, St.Albans, Herts, AL3 6EU, 1.0 edition.
- Bostock, E., Muller, R., and Kubie, J. (1991). Experience-dependent modifications of hippocampal place cell firing. *Hippocampus*, 1(2):193–205.
- Dahmen, H. (1980). A simple apparatus to investigate the orientation of walking insects. *Experientia*, 36:685–687.
- Dowding, J. and Murphy, E. (1994). Ecology of ship rats (*rattus rattus*) in a lauri (*agatis australis*) forest in northland, new zealnd. *New Zealand Journal of Ecology*, 18:19–28.
- Ebbinghaus, H. (1885). *Über das Gedächtnis: Untersuchungen zur experimentellen Psychologie*. Wissenschaftliche Buchgesellschaft, Darmstadt, 1 edition.

- Fox, S. and Ranck, J. (1981). Electrophysiological characteristics of hippocampal complex-spike cells and theta cells. *Exp Brain Res*, 41(3-4):399–410.
- Geary, D. and Huffman, K. (2002). Brain and cognitive evolution: forms of modularity and functions of mind. *Psychol Bull*, 128(5):667–698.
- Harvey, C., Collman, F., Dombeck, D., and Tank, D. (2009). Intracellular dynamics of hippocampal place cells during virtual navigation. *Nature*, 461(7266):941–946.
- Hassenstein, B. (1961). Wie sehen insekten bewegungen? *Naturwissenschaften*, 7:207–214.
- Hayman, R., Donnett, J., and Jeffery, K. (2008). The fuzzy-boundary arena—a method for constraining an animal’s range in spatial experiments without using walls. *J Neurosci Methods*, 167(2):184–190.
- Hayman, R., S.Chakraborty, Anderson, M., and Jeffery, K. (2003). Context-specific acquisition of location discrimination by hippocampal place cells. *Eur J Neurosci*, 18(10):2825–2834.
- Hirschmann, J. (2009). Behavioural and physiological responses of rats to acoustic boundaries. Master’s thesis, Graduate School of Neural & Behavioural Sciences, International Max Planck Research School, University of Tuebingen.
- Hölscher, C., Schnee, A., Dahmen, H., Setia, L., and Mallot, H. A. (2005). Rats are able to navigate in virtual environments. *J Exp Biol*, 208(Pt 3):561–569.
- Jovalekic, A. (2008). Neuronale grundlagen der raumrepräsentation bei nagern - eine verhaltensstudie in virtuellen umgebungen. Master’s thesis, University of Tuebingen.
- Jung, M. W., Wiener, S. I., and McNaughton, B. L. (1994). Comparison of spatial firing characteristics of units in dorsal and ventral hippocampus of the rat. *J Neurosci*, 14(12):7347–7356.
- Kentros, C., Agnihotri, N., Streater, S., Hawkins, R., and Kandel, E. (2004). Increased attention to spatial context increases both place field stability and spatial memory. *Neuron*, 42(2):283–295.

- Knierim, J. J., Kudrimoti, H. S., and McNaughton, B. L. (1995). Place cells, head direction cells, and the learning of landmark stability. *J Neurosci*, 15(3 Pt 1):1648–1659.
- Leutgeb, S., Leutgeb, J., Barnes, C., Moser, E., McNaughton, B., and Moser, M.-B. (2005). Independent codes for spatial and episodic memory in hippocampal neuronal ensembles. *Science*, 309(5734):619–623.
- Lever, C., Burgess, N., Cacucci, F., Hartley, T., and O’Keefe, J. (2002). What can the hippocampal representation of environmental geometry tell us about hebbian learning? *Biol Cybern*, 87(5-6):356–372.
- Libchik (2008). *On the Building of Microdrives*. Lab Rotation Project Summary University. Lab Rotation Project Summary University.
- Lubenov, E. V. and Siapas, A. G. (2009). Hippocampal theta oscillations are travelling waves. *Nature*, 459(7246):534–539.
- Maurer, A. P., Vanrhoads, S. R., Sutherland, G. R., Lipa, P., and McNaughton, B. L. (2005). Self-motion and the origin of differential spatial scaling along the septo-temporal axis of the hippocampus. *Hippocampus*, 15(7):841–852.
- Merriam-Webster, editor (2007). *Merriam-Webster’s Dictionary and Thesaurus*. Merriam-Webster.
- Muller, R. and Kubie, J. (1987). The effects of changes in the environment on the spatial firing of hippocampal complex-spike cells. *J Neurosci*, 7(7):1951–1968.
- O’Keefe, J. and Burgess, N. (1996). Geometric determinants of the place fields of hippocampal neurons. *Nature*, 381(6581):425–428.
- O’Keefe, J. and Dostrovsky, J. (1971). The hippocampus as a spatial map. preliminary evidence from unit activity in the freely-moving rat. *Brain Res*, 34(1):171–175.
- Paxinos, G. and Watson, C. (1998). *The Rat Brain in Stereotaxic Coordinates*. Academic Press.

- Ranck, J. B. (1973). Studies on single neurons in dorsal hippocampal formation and septum in unrestrained rats. i. behavioral correlates and firing repertoires. *Exp Neurol*, 41(2):461–531.
- Sales, G., Wilson, K., Spencer, K., and Milligan, S. (1988). Environmental ultrasound in laboratories and animal houses: a possible cause for concern in the welfare and use of laboratory animals. *Lab Anim*, 22(4):369–375.
- Schnee, A. (2008). *Rats in Virtual Reality: The Development of an Advanced Method to Study Animal Behaviour*. PhD thesis, University of Tuebingen.
- Tolman, E. (1948). Cognitive maps in rats and men. *Psychol Rev*, 55(4):189–208.
- Vail, M. L. (1976). Survival of some photoreceptor cells in albino rats following long-term exposure to continuous light. *Invest Ophthalmol*, 15(1):64–70.

Appendix A

Circuit Diagrams for the Headstage

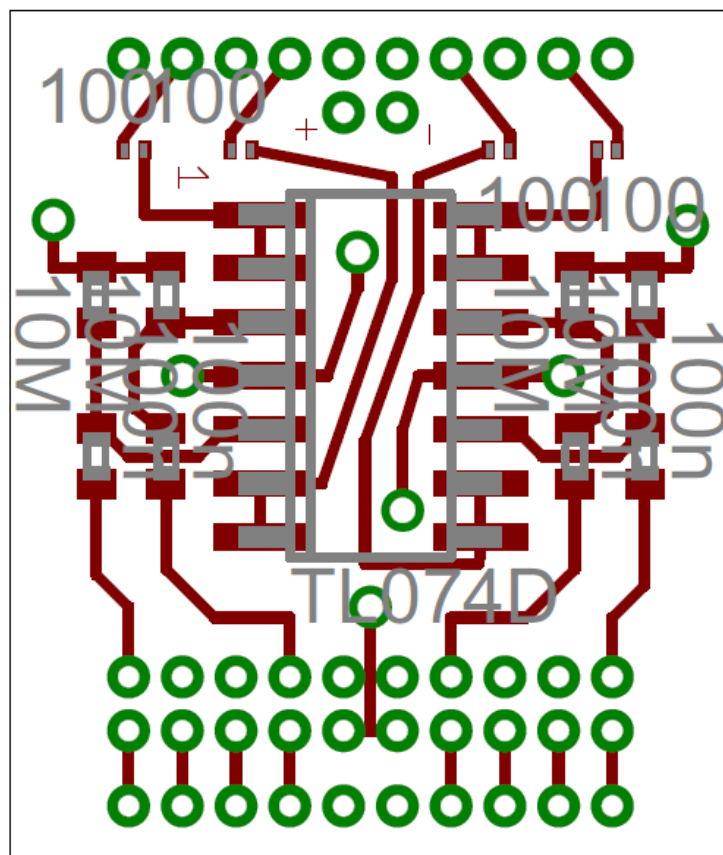


Figure A.1: Layout of circuit board I (top)

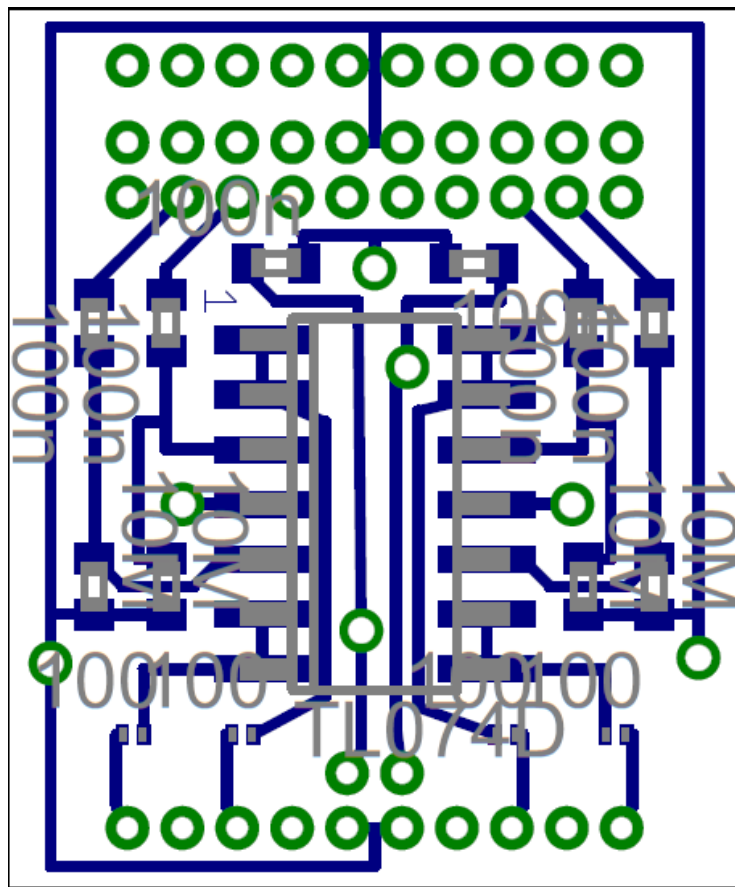


Figure A.2: Layout of circuit board I (bottom)

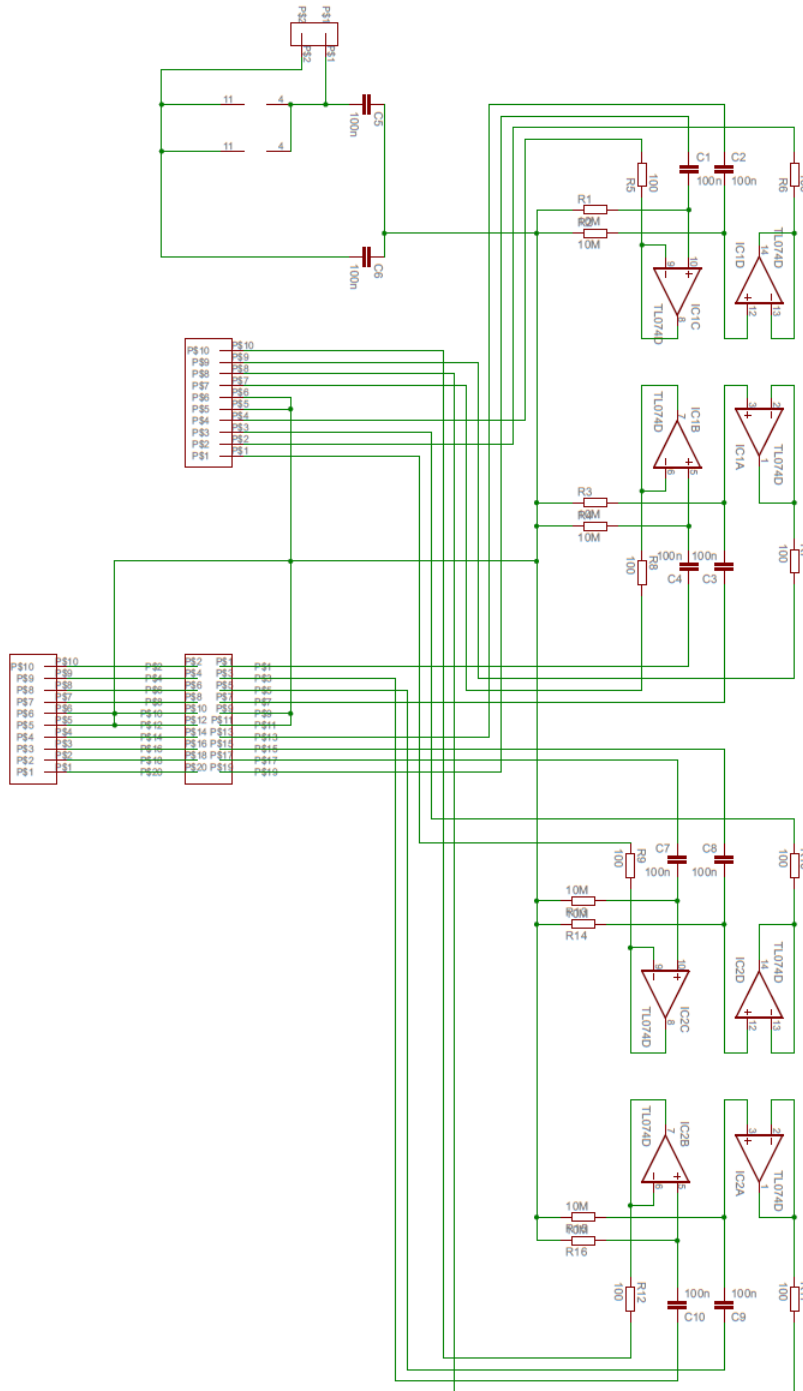


Figure A.3: Schematic view of circuit board I (with precision male connector for the cable to the preamplifier)

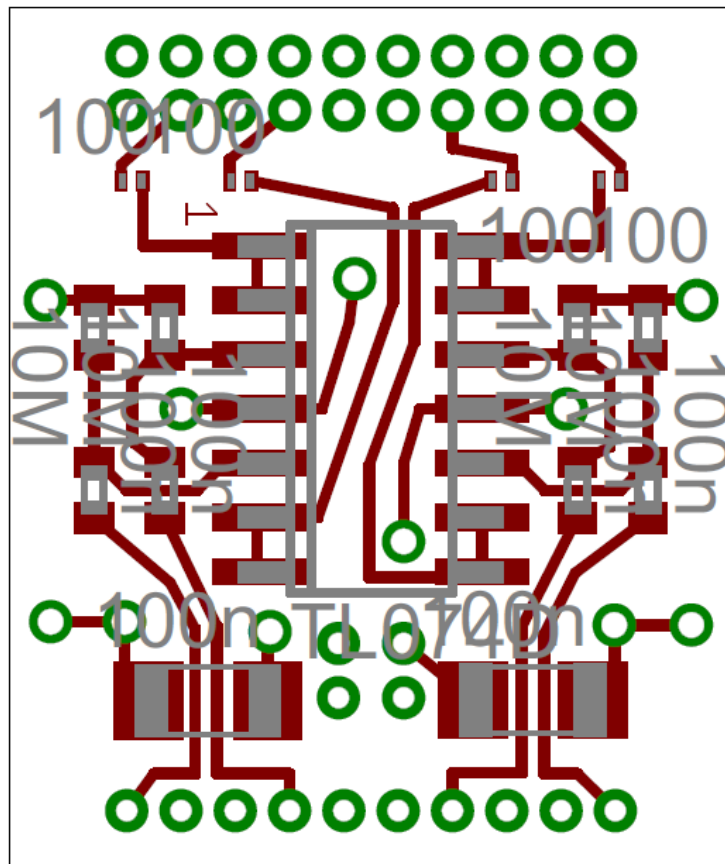


Figure A.4: Layout of circuit board II (top)

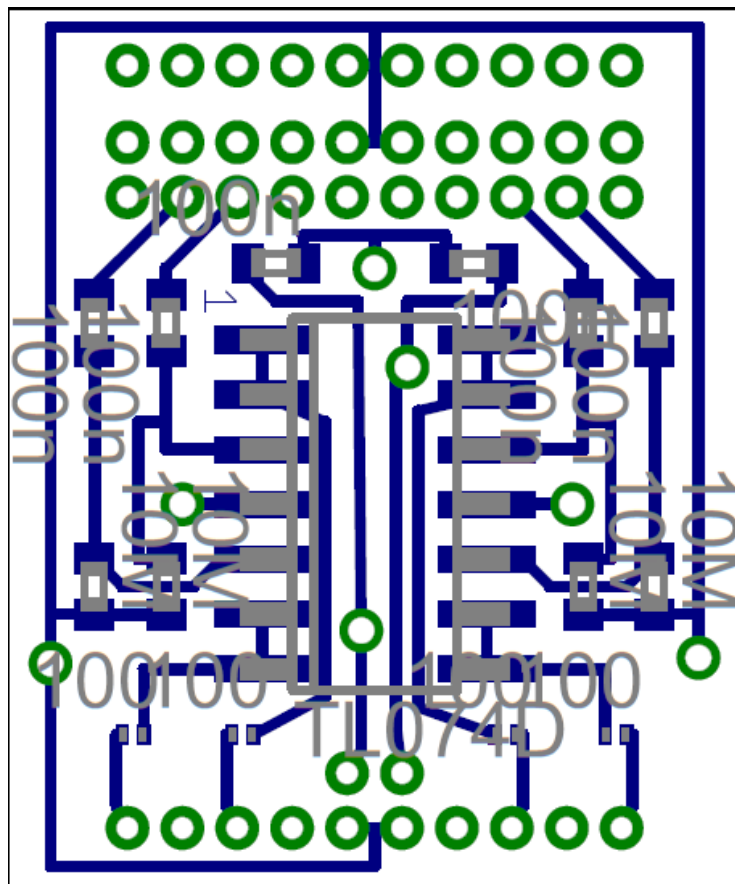


Figure A.5: Layout of circuit board II (bottom)

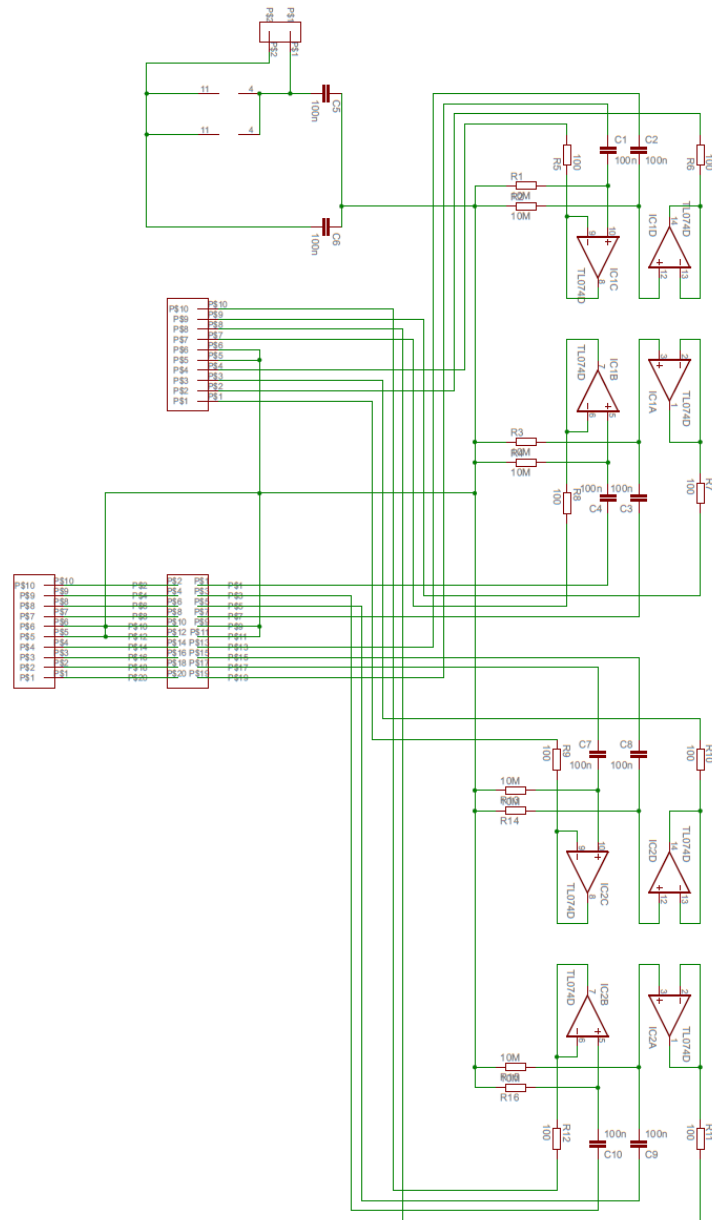


Figure A.6: Schematic view of circuit board II (with precision female connector for the microdrive)